Efficient Fault Tolerant Estimation using the IMM Methodology

ILIA RAPOPORT

YAAKOV OSHMAN, Fellow, IEEE
Technion–Israel Institute of Technology

Space systems are characterized by a low-intensity process noise resulting from uncertain forces and moments. In many cases, their scalar measurement channels can be assumed to be independent, with one-dimensional internal dynamics. The nominal operation of these systems can be severely damaged by faults in the sensors. A natural method that can be used to yield fault tolerant estimates of such systems is the interacting multiple model (IMM) filtering algorithm, which is known to provide very accurate results. However, having been derived for a general class of systems with switching parameters, the IMM filter does not utilize the independence of the measurement errors in different channels, nor does it exploit the fact that the process noise is of low intensity. Thus, the implementation of the IMM in this case is computationally expensive. A new estimation technique is proposed herein, that explicitly utilizes the aforementioned properties. In the resulting estimation scheme separate measurement channels are handled separately, thus reducing the computational complexity. It is shown that, whereas the IMM complexity is exponential in the number of fault-prone measurements, the complexity of the proposed technique is polynomial. A simulation study involving spacecraft attitude estimation is carried out. This study shows that the proposed technique closely approximates the full-blown IMM algorithm, while requiring only a modest fraction of the computational cost.

Manuscript received November 17, 2004; revised May 30, 2006; released for publication July 6, 2006.

IEEE Log No. T-AES/43/2/903006.

Refereeing for this contribution was handled by P. K. Willett.

This paper was presented at the AIAA *Guidance, Navigation and Control Conference*, Providence, RI, Aug. 16–19, 2004 (Paper AIAA-2004-5417).

Authors' address: Dept. of Aerospace Engineering, Technion–Israel Institute of Technology, Haifa 32000, Israel, E-mails: (yaakov.oshman@technion.ac.il), (iha.rapoport@gmail.com).

I. INTRODUCTION

Space missions involving precise pointing and/or spacecraft rendezvous require highly accurate data, which, in turn, has to be based on very accurate estimates of the spacecraft attitude and/or position. Operation in space is usually characterized by low-intensity uncertain forces and moments applied to the spacecraft. These inputs can be modeled as process noises.

Estimation accuracy can be severely damaged by measurement faults, which can take the form of measurement biases or noises (white or colored). Thus, GPS jamming and spoofing takes, in general, the form of colored noise and appears suddenly whenever it is activated [1]. Magnetometer faults, which are caused by magnetic fields generated by spacecraft electronics and electromagnetic torquing coils, usually take the form of biases (see [2, p. 251]) and appear whenever the corresponding current starts. Rate gyro faults, caused by input accelerations if the gyro gimbals are not perfectly balanced, are usually also modeled as biases (see [2, p. 198]) and appear whenever the spacecraft accelerates. So-called soft faults, in which case the faulty measurement errors are of the same order of magnitude as the nominal measurement noises, present a special and difficult problem. When measurements faults are caused by internal problems in the corresponding data channels, as in the aforementioned examples, the faults in separate channels can be assumed to be statistically independent. Moreover, measurement faults do not contaminate the main system dynamics, i.e., the spacecraft motion.

A popular approach to model such fault-prone behavior is by means of hybrid systems or systems with switching parameters [3]. One of the switching parameter values corresponds in these applications to the nominal system operation, whereas the others represent various fault situations [1, 4]. In systems with several independent fault-prone sensors and fault-free main dynamics, such as spacecraft, this general model can be simplified: the faults in different measurement channels can be modeled as separate Markovian Bernoulli random processes, where "1" designates a fault situation and "0" designates a nominal (fault-free) situation in the particular channel. Moreover, the dynamics of faulty measurements errors, like measurement biases (e.g., gyro drifts) and measurement noises (e.g., GPS jamming) can be usually represented by simple scalar linear systems, depending, in general, on the particular fault status.

It is well known that the optimal filtering algorithm for hybrid systems, that provides the estimates of the state vector and the switching parameters, requires infinite computation resources [5]. Therefore, a variety of suboptimal techniques was proposed [3, 6–10]. These methods are known in the literature as multiple model methods.

The most popular one is the interacting multiple model (IMM) algorithm [8]. The IMM runs in parallel a bank of Kalman filters (KFs), each of which corresponds to a certain system mode. At the heart of the IMM algorithm is a mixing procedure, performed in order to take into account the effect of mode switching on the state estimates. Originally conceived for tracking problems, the IMM algorithm was then used in the area of fault detection [4]. The accuracy of the IMM algorithm is well known and has been reported in many applications. However, straightforwardly implemented, this algorithm does not utilize the special features of the problem mentioned above, namely, the low intensity of the process noise, the statistical independence of separate measurement channels, and the a priori independence of the faults and the main system dynamics. As a result, the IMM algorithm is computationally expensive. For example, in a system with 5 independent measurement faults, there are $2^5 = 32$ possible modes, and, therefore, 32 parallel filters are required. In particular, the computational burden associated with the mixing step is especially high. A popular way to overcome the problem is to assume a small number of simultaneous faults [4].

Several methods try, in some sense, to exploit the measurement channel independence. In the federated filtering architecture [11] a separate KF runs for each measurement channel, producing the so-called local estimate. In this architecture, fault detection is performed via examining each of the local estimates, whereas the global state estimate, which is based on all of the measurements, is obtained by merging the local estimates and taking into account the detected faults. The disadvantages of this method are that 1) it does not take into account the Markovian property of the faults, and 2) it is not applicable to systems that are unobservable through each of the separate scalar measurement channels. The complementary filtering architecture [12], in which each of the local KFs takes into account all channels except one, is heavily based on the assumption of a single fault at a time.

An intuitive attempt to simplify the estimation scheme using the aforementioned properties has been recently presented in [13]. The proposed method requires to run in parallel a single state filter and a bank of separate fault estimators, one for each measurement channel. However, this method is restricted to the case of faulty measurement biases. Moreover, these biases are not estimated. Instead, the contribution of each channel to the state estimate is reduced according to the estimated probability of the corresponding fault.

A new fault-tolerant estimation scheme is proposed here. The approach is based on the fact that in a system with independent measurement channels and low process noise, the faulty measurement errors, conditioned on the main state variables, remain independent after measurement update. This property permits handling the measurement errors separately, thus reducing the computational burden. The corresponding fault tolerant filter is derived and compared with the ordinary IMM algorithm both in terms of computational complexity and estimation accuracy. It turns out that the proposed filter requires significantly less computational resources than the ordinary IMM. Specifically, it is shown that the complexity of the proposed technique is polynomial in the number of fault-prone measurements, whereas the IMM complexity is exponential. Furthermore, a spacecraft attitude estimation example, comparing the performance of the new algorithm to that of the ordinary IMM, is used to demonstrate that this computational saving does not come at the price of estimation performance.

The remainder of this paper is organized as follows. The system model is defined in Section II. For completeness, the ordinary IMM algorithm is then summarized in Section III. The underlying principles of the proposed filter, its derivation and the algorithm summary are presented in Section IV. The computational complexity analysis, comparing the new algorithm with the ordinary IMM, is presented in Section V. A numerical example, involving spacecraft attitude estimation, that compares the performance of the proposed technique to that of the ordinary IMM algorithm, is presented in Section VI. Concluding remarks are offered in the last section. For presentation clarity, proofs of several auxiliary results are deferred to appendices. As a matter of notational convention, lower case and upper case letters are used to denote random variables and their realizations, respectively.

II. PROBLEM FORMULATION

Consider an ordinary linear Gaussian state space model

$$x_{k+1} = \Phi_{k+1}x_k + \Psi_{k+1}u_{k+1} + G_{k+1}w_{k+1}, \qquad x_k \in \mathbb{R}^n \tag{1}$$

where $\{u_k\}_{k=1}^{\infty}$ is a sequence of (known) deterministic inputs, $\{w_k\}_{k=1}^{\infty}$ is Gaussian white sequence of the main process noise with $w_k \sim \mathcal{N}(0, Q_k)$, and $x_0 \sim \mathcal{N}(\hat{x}_0, \Sigma_0)$ is the random initial state with $\Sigma_0 > 0$. The state transition matrix Φ_k is assumed to be nonsingular. The system is observed through m independent channels, each of which produces scalar measurements. A fault can occur in each of these channels. The measurement equations are given by

$$y_k^{(i)} = h_k^{(i)^T} x_k + c_k^{(i)}(\gamma_k^{(i)})b_k^{(i)} + v_k^{(i)}, \qquad i = 1,2,\ldots,m \tag{2}$$

where $\{v_k^{(i)}\}_{k=1}^{\infty}$ are independent Gaussian white sequences of measurement noises with $v_k^{(i)} \sim \mathcal{N}(0, R_k^{(i)})$ and $R_k^{(i)} > 0$, $\{\gamma_k^{(i)}\}_{k=0}^{\infty}$ is a Bernoulli Markov chain

of fault indicators, and $b_k^{(i)}$ is a faulty measurement error. The distribution of the fault indicator sequence is described by the following initial and transition probabilities:

$$\Pr\{\gamma_0^{(i)} = 1\} = \Pi_0^{(i)} \tag{3a}$$

$$\Pr\{\gamma_{k+1}^{(i)} = 1 \mid \gamma_k^{(i)} = j\} = P_{1j}^{(i)}(k+1 \mid k), \qquad j \in \{0,1\}. \tag{3b}$$

Each of the scalar processes $\{b_k^{(i)}\}_{k=0}^{\infty}$ is described by the following dynamics equation

$$b_{k+1}^{(i)} = a_{k+1}^{(i)}(\gamma_{k+1}^{(i)})b_k^{(i)} + g_{k+1}^{(i)}(\gamma_{k+1}^{(i)})\tilde{w}_{k+1}^{(i)} \tag{4}$$

where $\{\tilde{w}_k^{(i)}\}_{k=1}^{\infty}$ are independent Gaussian white sequences with $\tilde{w}_k^{(i)} \sim \mathcal{N}(0, q_k^{(i)})$. It is assumed that x_0, $\{w_k\}_{k=1}^{\infty}$, $\{\gamma_k^{(i)}\}_{k=0}^{\infty}$, $\{v_k^{(i)}\}_{k=1}^{\infty}$, $\{\tilde{w}_k^{(i)}\}_{k=1}^{\infty}$ and $b_0^{(i)}$ are mutually independent. For notational simplicity the explicit time dependence is suppressed in the sequel in all places where it is clear by context.

The main emphasis in this work is on space-related systems, typically characterized by the low uncertainty about their main dynamics. Therefore, the following assumption is made.

Assumption 1 The intensity of the main process noise $\{w_k\}_{k=1}^{\infty}$ in (1) is low, i.e., the matrices Q_k take small values.

The model addressed in this work can describe a wide class of fault-prone measurement systems. Thus, $a^{(i)}(\gamma) \equiv 1$, $g^{(i)}(\gamma) \equiv 0$ and $c^{(i)}(\gamma) \equiv 1$ correspond to a system with permanent measurement biases; a system with faulty measurement biases that change their value each time they appear can be modeled using

$$\begin{aligned} a^{(i)}(\gamma) = c^{(i)}(\gamma) &= \begin{cases} 0 & \text{for} \quad \gamma = 0 \\ 1 & \text{for} \quad \gamma = 1 \end{cases} \\ g^{(i)}(\gamma) &= \begin{cases} 1 & \text{for} \quad \gamma = 0 \\ 0 & \text{for} \quad \gamma = 1 \end{cases} \end{aligned} \tag{5}$$

and $a^{(i)}(\gamma) \equiv 0$, $g^{(i)}(\gamma) \equiv 1$ and $c^{(i)}$ as in (5) yield a system with additive faulty white noises.

The goal of this work is to derive a minimum mean square error (MMSE) estimation algorithm for the states and fault indicators of the system.

The following definitions are used in the sequel:

$$y_k \triangleq [y_k^{(1)}, y_k^{(2)}, \ldots, y_k^{(m)}]^T \tag{6a}$$

$$\mathcal{Y}_k \triangleq [y_1^T, y_2^T, \ldots, y_k^T]^T \tag{6b}$$

$$b_k \triangleq [b_k^{(1)}, b_k^{(2)}, \ldots, b_k^{(m)}]^T \tag{6c}$$

$$\gamma_k \triangleq [\gamma_k^{(1)}, \gamma_k^{(2)}, \ldots, \gamma_k^{(m)}]^T. \tag{6d}$$

For completeness, the IMM algorithm is reviewed next.

III. REVIEW OF IMM ALGORITHM

Consider a hybrid system

$$x_k = A_k(\theta_k)x_{k-1} + B_k(\theta_k)w_k, \qquad x_k \in \mathbb{R}^n \tag{7}$$

with observations

$$y_k = H_k(\theta_k)x_k + v_k, \qquad y_k \in \mathbb{R}^m \tag{8}$$

where the processes $\{w_k\}_{k=0}^{\infty}$ and $\{v_k\}_{k=0}^{\infty}$ are mutually independent Gaussian white noises with $w_k \sim \mathcal{N}(0, Q_k)$, $v_k \sim \mathcal{N}(0, R_k(\theta_k))$, and $\{\theta_k\}_{k=0}^{\infty}$ is a Markov chain taking values in $\{1, 2, \ldots, S\}$ according to the transition probabilities

$$P_{ij}(k \mid k-1) \triangleq \Pr\{\theta_k = i \mid \theta_{k-1} = j\}. \tag{9}$$

The posterior state distribution can be exactly computed via the following five steps:

1) Mode evolution: $\theta_k \mid \mathcal{Y}_k \Rightarrow \theta_{k+1} \mid \mathcal{Y}_k$,
2) State mixing: $x_k \mid \theta_k, \mathcal{Y}_k \Rightarrow x_k \mid \theta_{k+1}, \mathcal{Y}_k$,
3) State evolution: $x_k \mid \theta_{k+1}, \mathcal{Y}_k \Rightarrow x_{k+1} \mid \theta_{k+1}, \mathcal{Y}_k$,
4) Mode measurement update: $\theta_{k+1} \mid \mathcal{Y}_k \Rightarrow \theta_{k+1} \mid \mathcal{Y}_{k+1}$,
5) State measurement update: $x_{k+1} \mid \theta_{k+1}, \mathcal{Y}_k \Rightarrow x_{k+1} \mid \theta_{k+1}, \mathcal{Y}_{k+1}$.

The IMM algorithm [8] is based on the assumption that the distribution $x_{k+1} \mid \theta_{k+1}, \mathcal{Y}_k$ resulting from Step 3 is Gaussian. This assumption permits representing the distributions $x_{k+1} \mid \theta_{k+1}, \mathcal{Y}_k$ and $x_{k+1} \mid \theta_{k+1}, \mathcal{Y}_{k+1}$ by their mean vectors and covariance matrices. Denote

$$p_{k|l}(i) \triangleq \Pr\{\theta_k = i \mid \mathcal{Y}_l\} \tag{10}$$

$$\hat{x}_{k|r,l}(i) \triangleq E[x_k \mid \theta_r = i, \mathcal{Y}_l] \tag{11}$$

$$\hat{P}_{k|r,l}(i) \triangleq \operatorname{cov}[x_k \mid \theta_r = i, \mathcal{Y}_l]. \tag{12}$$

Then, a complete cycle of the IMM algorithm comprises the following steps:

1) Mode evolution, $\theta_k \mid \mathcal{Y}_k \Rightarrow \theta_{k+1} \mid \mathcal{Y}_k$:

$$p_{k+1|k}(i) = \sum_{j=1}^{S} P_{ij}(k+1 \mid k)p_{k|k}(j) \tag{13}$$

for $i = 1, 2, \ldots, S$.

2) State mixing, $x_k \mid \theta_k, \mathcal{Y}_k \Rightarrow x_k \mid \theta_{k+1}, \mathcal{Y}_k$:

$$\hat{x}_{k|k+1,k}(i) = \sum_{j=1}^{S} \mu_{ij}\hat{x}_{k|k,k}(j) \tag{14a}$$

$$\begin{aligned} \hat{P}_{k|k+1,k}(i) = \sum_{j=1}^{S} \mu_{ij}(&\hat{P}_{k|k,k}(j) + [\hat{x}_{k|k,k}(j) - \hat{x}_{k|k+1,k}(i)] \\ &\times [\hat{x}_{k|k,k}(j) - \hat{x}_{k|k+1,k}(i)]^T) \end{aligned} \tag{14b}$$

for $i = 1,2,\ldots,S$, where the mixing probabilities μ_{ij} are given by

$$\mu_{ij} = \frac{P_{ij}(k+1 \mid k)p_{k|k}(j)}{p_{k+1|k}(i)}. \tag{15}$$

3) State evolution, $x_k \mid \theta_{k+1}, \mathcal{Y}_k \Rightarrow x_{k+1} \mid \theta_{k+1}, \mathcal{Y}_k$:

$$\hat{x}_{k+1|k+1,k}(i) = A_{k+1}(i)\hat{x}_{k|k+1,k}(i) \tag{16a}$$

$$\hat{P}_{k+1|k+1,k}(i) = A_{k+1}(i)\hat{P}_{k|k+1,k}(i)A_{k+1}(i)^T + B_{k+1}(i)Q_{k+1}B_{k+1}(i)^T \tag{16b}$$

for $i = 1,2,\ldots,S$.

4) Mode measurement update, $\theta_{k+1} \mid \mathcal{Y}_k \Rightarrow \theta_{k+1} \mid \mathcal{Y}_{k+1}$:

$$p_{k+1|k+1}(i) = \frac{f_i p_{k+1|k}(i)}{\sum_{j=1}^{S} f_j p_{k+1|k}(j)} \tag{17}$$

for $i = 1,2,\ldots,S$, where

$$f_i = \frac{1}{\sqrt{(2\pi)^m \det S_i}} \exp\left(-\frac{1}{2}\tilde{y}_i^T S_i^{-1} \tilde{y}_i\right) \tag{18}$$

and

$$\tilde{y}_i = y_{k+1} - H_{k+1}(i)\hat{x}_{k+1|k+1,k}(i) \tag{19a}$$

$$S_i = H_{k+1}(i)\hat{P}_{k+1|k+1,k}(i)H_{k+1}(i)^T + R_{k+1}(i). \tag{19b}$$

5) State measurement update, $x_{k+1} \mid \theta_{k+1}, \mathcal{Y}_k \Rightarrow x_{k+1} \mid \theta_{k+1}, \mathcal{Y}_{k+1}$:

$$\hat{x}_{k+1|k+1,k+1}(i) = \hat{x}_{k+1|k+1,k}(i) + K_i \tilde{y}_i \tag{20a}$$

$$\hat{P}_{k+1|k+1,k+1}(i) = (I - K_i H_{k+1}(i))\hat{P}_{k+1|k+1,k}(i) \tag{20b}$$

for $i = 1,2,\ldots,S$, where

$$K_i = \hat{P}_{k+1|k+1,k}(i)H_{k+1}(i)^T S_i^{-1} \tag{21}$$

and $\tilde{y}_i$ as well as S_i are defined in (19).

For output purposes one can compute an estimate $\hat{x}_{k+1|k+1}$ of the state vector x_{k+1} as

$$\hat{x}_{k+1|k+1} = \sum_{i=1}^{S} \hat{x}_{k+1|k+1,k+1}(i)p_{k+1|k+1}(i). \tag{22}$$

REMARK 1 Steps 3 and 5 are, in fact, a bank of S KFs, each of which corresponds to a certain system mode.

IV. FILTERING ALGORITHM

A. Main Idea

The idea underlying the proposed estimation technique is based on the following property of the posterior state distribution, which in turn follows from Assumption 1.

PROPOSITION 1 *Under Assumption* 1*, the posterior distribution of the states x_k, $b_k^{(i)}$ and the fault indicators $\gamma_k^{(i)}$ can be written as*

$$p_{x_k,b_k,\gamma_k|\mathcal{Y}_k}(X_k,B_k,\Gamma_k \mid \Upsilon_k) = p_{x_k|\mathcal{Y}_k}(X_k \mid \Upsilon_k)\prod_{i=1}^{m}[p_{b_k^{(i)}|\gamma_k^{(i)},x_k,\mathcal{Y}_k}(B_k^{(i)} \mid \Gamma_k^{(i)},X_k,\Upsilon_k) \times \Pr\{\gamma_k^{(i)} = \Gamma_k^{(i)} \mid x_k = X_k, \mathcal{Y}_k = \Upsilon_k\}] \tag{23a}$$

$$p_{x_k,b_{k+1},\gamma_{k+1}|\mathcal{Y}_k}(X_k,B_{k+1},\Gamma_{k+1} \mid \Upsilon_k) = p_{x_k|\mathcal{Y}_k}(X_k \mid \Upsilon_k) \times \prod_{i=1}^{m}[p_{b_{k+1}^{(i)}|\gamma_{k+1}^{(i)},x_k,\mathcal{Y}_k}(B_{k+1}^{(i)} \mid \Gamma_{k+1}^{(i)},X_k,\Upsilon_k) \times \Pr\{\gamma_{k+1}^{(i)} = \Gamma_{k+1}^{(i)} \mid x_k = X_k, \mathcal{Y}_k = \Upsilon_k\}] \tag{23b}$$

$$p_{x_{k+1},b_{k+1},\gamma_{k+1}|\mathcal{Y}_k}(X_{k+1},B_{k+1},\Gamma_{k+1} \mid \Upsilon_k) = p_{x_{k+1}|\mathcal{Y}_k}(X_{k+1} \mid \Upsilon_k) \times \prod_{i=1}^{m}[p_{b_{k+1}^{(i)}|\gamma_{k+1}^{(i)},x_{k+1},\mathcal{Y}_k}(B_{k+1}^{(i)} \mid \Gamma_{k+1}^{(i)},X_{k+1},\Upsilon_k) \times \Pr\{\gamma_{k+1}^{(i)} = \Gamma_{k+1}^{(i)} \mid x_{k+1} = X_{k+1}, \mathcal{Y}_k = \Upsilon_k\}] \tag{23c}$$

where $p_{x,b,\gamma|\mathcal{Y}}(X,B,\Gamma \mid \Upsilon)$ stands for $p_{x,b|\gamma,\mathcal{Y}}(X,B \mid \Gamma,\Upsilon)\Pr(\gamma = \Gamma \mid \mathcal{Y} = \Upsilon)$. In other words, given the main state vector x_k, the estimates of the parameters characterizing the faulty behavior of different measurement channels remain independent.

PROOF The proof is deferred to Appendix A.

To facilitate the derivation of a closed-form estimation algorithm, the following two assumptions, concerning the state posterior distribution properties, are now made.

Assumption 2 The distribution $x_{k+1}, b_{k+1} \mid \gamma_{k+1}, \mathcal{Y}_k$ is Gaussian.

Assumption 3 The estimates of the main state variables are independent of the estimates of the fault indicators: $x_k \mid \mathcal{Y}_k \perp\!\!\!\perp \gamma_k \mid \mathcal{Y}_k$.

Assumption 2 is nothing but the standard IMM assumption on the Gaussian distribution of the conditional state [8]. Assumption 3 is justified based on the following observation. Notice that the state variables are clearly divided into two sets. In the first set, which includes the main state vector x_k, the state dynamics does not depend on the fault behavior (see (1)). The contributions of these state variables to the measurements are also independent of the faults, as can be observed from (2). In the second set, which includes all measurement error variables $b_k^{(i)}$, the fault indicators do affect both the state dynamics and the contributions to the measurements. This observation leads to the conclusion that the main states remain less coupled with the fault indicators than the measurement error variables also after measurement updates.

Intuitively it can be concluded also that the coupling between the main states and the fault indicators weakens as the number of measurement channels increases.

Using these assumptions the following property of the state posterior distribution can now be stated.

PROPOSITION 2 *The following distributions, associated with the probability density functions (pdfs) appearing in the representation* (23)*, are Gaussian:*

1) $x_{k+1}, b_{k+1} \mid \gamma_{k+1}, \mathcal{Y}_{k+1}$,
2) $x_{k+1} \mid \mathcal{Y}_k$,
3) $x_{k+1} \mid \mathcal{Y}_{k+1}$,
4) $x_{k+1}, b_{k+1}^{(i)} \mid \gamma_{k+1}^{(i)}, \mathcal{Y}_k$,
5) $x_{k+1}, b_{k+1}^{(i)} \mid \gamma_{k+1}^{(i)}, \mathcal{Y}_{k+1}$.

PROOF The proof is deferred to Appendix B.

An immediate conclusion from Proposition 2 is that, for $l \in \{k, k+1\}$, the conditional distribution $b_{k+1}^{(i)} \mid \gamma_{k+1}^{(i)}, x_{k+1}, \mathcal{Y}_l$ can be represented as

$$b_{k+1}^{(i)} \mid \gamma_{k+1}^{(i)}, x_{k+1}, \mathcal{Y}_l \sim \mathcal{N}(\alpha + \beta^T (x_{k+1} - \hat{x}_{k+1|l}), \rho), \quad \beta \in \mathbb{R}^n \tag{24}$$

where the parameters α, β, and ρ are independent of x_{k+1} and

$$\hat{x}_{k+1|l} \triangleq E[x_{k+1} \mid \mathcal{Y}_l]. \tag{25}$$

Together with Propositions 1 and 2, this observation makes it possible to represent the posterior state distribution using the following parameters:

1) the mean and the covariance matrix of the distribution $x_{k+1} \mid \mathcal{Y}_l$,
2) the conditional probabilities $\Pr\{\gamma_{k+1}^{(i)} = 1 \mid \mathcal{Y}_l\}$,
3) the parameters α, β, and ρ of each of the distributions $b_{k+1}^{(i)} \mid \gamma_{k+1}^{(i)}, x_{k+1}, \mathcal{Y}_l$.

The idea underlying the proposed filter consists of the computation of the posterior state distribution using this set of parameters, rather than the parameters used in the ordinary IMM filter, which include 2^m mean vectors and covariance matrices of the augmented state vector conditioned on the system mode. Obviously, the number of parameters in the new representation is smaller than in the ordinary IMM algorithm. Notice also that in the new representation each fault is handled separately, unlike in the IMM algorithm, where all fault combinations must be treated. In Section V it will also be shown that Assumptions 1, 2, and 3, and the facts that 1) the dynamics equations of x and $b^{(i)}$ are uncoupled, 2) the measurement noises are independent, and 3) each measurement error state affects a separate channel, render this procedure less computationally demanding than the ordinary IMM algorithm.

The following notational convention is adopted in the sequel. In accordance with (25), the mean and the covariance matrix of the distribution $x_k \mid \mathcal{Y}_l$ are denoted by $\hat{x}_{k|l}$ and $\hat{P}_{k|l}$, respectively, that is

$$x_k \mid \mathcal{Y}_l \sim \mathcal{N}(\hat{x}_{k|l}, \hat{P}_{k|l}). \tag{26}$$

Next, let

$$\hat{\gamma}_{k|l}^{(i)} \triangleq \Pr\{\gamma_k^{(i)} = 1 \mid \mathcal{Y}_l\}. \tag{27}$$

Finally, the parameters α, β, and ρ of the conditional distribution $b_k^{(i)} \mid \gamma_r^{(i)} = j, x_m, \mathcal{Y}_l$ for $j \in \{0,1\}$ [see (24)] are denoted by $\alpha_{k|r,m,l}^{(i)}(j)$, $\beta_{k|r,m,l}^{(i)}(j)$, and $\rho_{k|r,m,l}^{(i)}(j)$, respectively, meaning that

$$E[b_k^{(i)} \mid \gamma_r^{(i)} = j, x_m, \mathcal{Y}_l] = \alpha_{k|r,m,l}^{(i)}(j) + \beta_{k|r,m,l}^{(i)\,T}(j)(x_m - \hat{x}_{m|l}) \tag{28a}$$

$$\operatorname{var}[b_k^{(i)} \mid \gamma_r^{(i)} = j, x_m, \mathcal{Y}_l] = \rho_{k|r,m,l}^{(i)}(j). \tag{28b}$$

A detailed derivation of the proposed algorithm is presented next.

B. Algorithm Derivation

The recursion cycle for the evolution of the state posterior distribution, given in the form (23), comprises two main steps: the time propagation step and the measurement update step. Since the equations describing the system time evolution are uncoupled for different channels, and due to Proposition 1, it is sufficient to track only the evolution of the distribution of $x_k, b_k^{(i)}, \gamma_k^{(i)} \mid \mathcal{Y}_k$ in order to derive the time propagation procedure. First, the time evolution of $\gamma_k^{(i)}$ is obtained by a direct application of the Chapman-Kolmogorov equation to m Markov chains $\{\gamma_k^{(i)}\}_{k=0}^{\infty}$. Also, according to Proposition 2, the conditional distribution $x_k, b_k^{(i)} \mid \gamma_k^{(i)}, \mathcal{Y}_k$ is Gaussian. Using the notation given in (26), (27), and (28) its parameters can be written as

$$E\left[\begin{bmatrix} x_k \\ b_k^{(i)} \end{bmatrix} \middle| \gamma_k^{(i)} = \xi, \mathcal{Y}_k\right] = \begin{bmatrix} \hat{x}_{k|k} \\ \alpha_{k|k,k,k}^{(i)}(\xi) \end{bmatrix} \tag{29a}$$

$$\operatorname{cov}\left[\begin{bmatrix} x_k \\ b_k^{(i)} \end{bmatrix} \middle| \gamma_k^{(i)} = \xi, \mathcal{Y}_k\right] = \begin{bmatrix} \hat{P}_{k|k} & \hat{P}_{k|k}\beta_{k|k,k,k}^{(i)}(\xi) \\ \beta_{k|k,k,k}^{(i)\,T}(\xi)\hat{P}_{k|k} & \rho_{k|k,k,k}^{(i)}(\xi) + \beta_{k|k,k,k}^{(i)\,T}(\xi)\hat{P}_{k|k}\beta_{k|k,k,k}^{(i)}(\xi) \end{bmatrix}. \tag{29b}$$

Defining

$$\mu_{\xi\eta} \triangleq \Pr\{\gamma_k^{(i)} = \eta \mid \gamma_{k+1}^{(i)} = \xi, \mathcal{Y}_k\} \tag{30}$$

the ordinary IMM mixing procedure yields

$$E\left[\begin{bmatrix} x_k \\ b_k^{(i)} \end{bmatrix} \middle| \gamma_{k+1}^{(i)} = \xi, \mathcal{Y}_k\right] = \sum_{\eta=0}^{1} \mu_{\xi\eta} E\left[\begin{bmatrix} x_k \\ b_k^{(i)} \end{bmatrix} \middle| \gamma_k^{(i)} = \eta, \mathcal{Y}_k\right] = \begin{bmatrix} \hat{x}_{k|k} \\ \alpha_{k|k+1,k,k}^{(i)}(\xi) \end{bmatrix} \tag{31}$$

where

$$\alpha^{(i)}_{k|k+1,k,k}(\xi) = \sum_{\eta=0}^{1} \mu_{\xi\eta}\alpha^{(i)}_{k|k,k,k}(\eta). \tag{32}$$

Similarly, defining

$$\beta^{(i)}_{k|k+1,k,k}(\xi) \triangleq \sum_{\eta=0}^{1} \mu_{\xi\eta}\beta^{(i)}_{k|k,k,k}(\eta) \tag{33}$$

noting that

$$\begin{aligned}
&\sum_{\eta=0}^{1} \mu_{\xi\eta}{\beta^{(i)}_{k|k,k,k}}^{T}(\eta)\hat{P}_{k|k}\beta^{(i)}_{k|k,k,k}(\eta) \\
&\quad = \sum_{\eta=0}^{1} \mu_{\xi\eta}{\beta^{(i)}_{k|k,k,k}}^{T}(\eta)\hat{P}_{k|k}(\beta^{(i)}_{k|k,k,k}(\eta) - \beta^{(i)}_{k|k+1,k,k}(\xi)) \\
&\qquad + {\beta^{(i)}_{k|k+1,k,k}}^{T}(\xi)\hat{P}_{k|k}\beta^{(i)}_{k|k+1,k,k}(\xi) \\
&\quad = \sum_{\eta=0}^{1} \mu_{\xi\eta}(\beta^{(i)}_{k|k,k,k}(\eta) - \beta^{(i)}_{k|k+1,k,k}(\xi))^T\hat{P}_{k|k} \\
&\qquad \times (\beta^{(i)}_{k|k,k,k}(\eta) - \beta^{(i)}_{k|k+1,k,k}(\xi)) \\
&\qquad + {\beta^{(i)}_{k|k+1,k,k}}^{T}(\xi)\hat{P}_{k|k}\beta^{(i)}_{k|k+1,k,k}(\xi)
\end{aligned} \tag{34}$$

and defining

$$\begin{aligned}
\rho^{(i)}_{k|k+1,k,k}(\xi) \triangleq \sum_{\eta=0}^{1} \mu_{\xi\eta}[&\rho^{(i)}_{k|k,k,k}(\eta) + (\alpha^{(i)}_{k|k,k,k}(\eta) - \alpha^{(i)}_{k|k+1,k,k}(\xi))^2 \\
&+ (\beta^{(i)}_{k|k,k,k}(\eta) - \beta^{(i)}_{k|k+1,k,k}(\xi))^T\hat{P}_{k|k}(\beta^{(i)}_{k|k,k,k}(\eta) \\
&- \beta^{(i)}_{k|k+1,k,k}(\xi))]
\end{aligned} \tag{35}$$

yields

$$\begin{aligned}
&\operatorname{cov}\left[\begin{bmatrix} x_k \\ b^{(i)}_k \end{bmatrix} \middle| \gamma^{(i)}_{k+1} = \xi, \mathcal{Y}_k\right] \\
&= \begin{bmatrix} \hat{P}_{k|k} & \hat{P}_{k|k}\beta^{(i)}_{k|k+1,k,k}(\xi) \\ {\beta^{(i)}_{k|k+1,k,k}}^{T}(\xi)\hat{P}_{k|k} & \rho^{(i)}_{k|k+1,k,k}(\xi) + {\beta^{(i)}_{k|k+1,k,k}}^{T}(\xi)\hat{P}_{k|k}\beta^{(i)}_{k|k+1,k,k}(\xi) \end{bmatrix}.
\end{aligned} \tag{36}$$

Now, the system dynamics equations (1) and (4) yield

$$E\left[\begin{bmatrix} x_{k+1} \\ b^{(i)}_{k+1} \end{bmatrix} \middle| \gamma^{(i)}_{k+1} = \xi, \mathcal{Y}_k\right] = \begin{bmatrix} \hat{x}_{k+1|k} \\ \alpha^{(i)}_{k+1|k+1,k,k}(\xi) \end{bmatrix} \tag{37}$$

where

$$\hat{x}_{k+1|k} = \Phi\hat{x}_{k|k} + \Psi u_{k+1} \tag{38a}$$

$$\alpha^{(i)}_{k+1|k+1,k,k}(\xi) = a^{(i)}(\xi)\alpha^{(i)}_{k|k+1,k,k}(\xi) \tag{38b}$$

and

$$\operatorname{cov}\left[\begin{bmatrix} x_k \\ b^{(i)}_k \end{bmatrix} \middle| \gamma^{(i)}_{k+1} = \xi, \mathcal{Y}_k\right] = \begin{bmatrix} \hat{P}_{k+1|k} & \Phi\hat{P}_{k|k}\beta^{(i)}_{k+1|k+1,k,k}(\xi) \\ {\beta^{(i)}_{k+1|k+1,k,k}}^{T}(\xi)\hat{P}_{k|k}\Phi^T & \rho^{(i)}_{k+1|k+1,k,k}(\xi) + {\beta^{(i)}_{k+1|k+1,k,k}}^{T}(\xi)\hat{P}_{k|k}\beta^{(i)}_{k+1|k+1,k,k}(\xi) \end{bmatrix} \tag{39}$$

where

$$\hat{P}_{k+1|k} = \Phi\hat{P}_{k|k}\Phi^T + GQG^T \tag{40a}$$

$$\beta^{(i)}_{k+1|k+1,k,k}(\xi) = a^{(i)}(\xi)\beta^{(i)}_{k|k+1,k,k}(\xi) \tag{40b}$$

$$\rho^{(i)}_{k+1|k+1,k,k}(\xi) = {a^{(i)}}^2(\xi)\rho^{(i)}_{k|k+1,k,k}(\xi) + {g^{(i)}}^2(\xi)q^{(i)}(\xi). \tag{40c}$$

Concluding the time propagation step, notice that, according to Proposition 2, the distribution $x_{k+1}, b^{(i)}_{k+1} \mid \gamma^{(i)}_{k+1}, \mathcal{Y}_k$ is Gaussian. Moreover, according to Assumption 3, given the measurement history $\mathcal{Y}_k$, x_{k+1} and $\gamma^{(i)}_{k+1}$ are independent. Therefore, using the parameters defined in (26),

$$x_{k+1} \mid \mathcal{Y}_k \sim \mathcal{N}(\hat{x}_{k+1|k}, \hat{P}_{k+1|k}) \tag{41}$$

and

$$\begin{aligned}
b^{(i)}_{k+1} \mid \gamma^{(i)}_{k+1} = \xi, x_{k+1}, \mathcal{Y}_k \\
\sim \mathcal{N}(\alpha^{(i)}_{k+1|k+1,k+1,k}(\xi) + {\beta^{(i)}_{k+1|k+1,k+1,k}}^{T}(\xi) \\
\times (x_{k+1} - \hat{x}_{k+1|k}), \rho^{(i)}_{k+1|k+1,k+1,k}(\xi))
\end{aligned} \tag{42}$$

where

$$\alpha^{(i)}_{k+1|k+1,k+1,k}(\xi) = \alpha^{(i)}_{k+1|k+1,k,k}(\xi) \tag{43a}$$

$$\beta^{(i)}_{k+1|k+1,k+1,k}(\xi) = \hat{P}^{-1}_{k+1|k}\Phi\hat{P}_{k|k}\beta^{(i)}_{k+1|k+1,k,k}(\xi) \tag{43b}$$

$$\begin{aligned}
\rho^{(i)}_{k+1|k+1,k+1,k}(\xi) &= \rho^{(i)}_{k+1|k+1,k,k}(\xi) + {\beta^{(i)}_{k+1|k+1,k,k}}^{T}(\xi) \\
&\quad \times (\hat{P}_{k|k} - \hat{P}_{k|k}\Phi^T\hat{P}^{-1}_{k+1|k}\Phi\hat{P}_{k|k})\beta^{(i)}_{k+1|k+1,k,k}(\xi) \\
&= \rho^{(i)}_{k+1|k+1,k,k}(\xi) + {\beta^{(i)}_{k+1|k+1,k,k}}^{T}(\xi) \\
&\quad \times \hat{P}_{k|k}\beta^{(i)}_{k+1|k+1,k,k}(\xi) - {\beta^{(i)}_{k+1|k+1,k+1,k}}^{T}(\xi) \\
&\quad \times \hat{P}_{k+1|k}\beta^{(i)}_{k+1|k+1,k+1,k}(\xi).
\end{aligned} \tag{43c}$$

The measurement update step is based on the following observations.

PROPOSITION 3 *Let x, $y^{(1)}$, $y^{(2)}, \ldots, y^{(r)}$ be random vectors satisfying*

$$p_{y^{(1)},y^{(2)},\ldots,y^{(r)}|x}(Y^{(1)}, Y^{(2)}, \ldots, Y^{(r)} \mid X) = \prod_{i=1}^{r} p_{y^{(i)}|x}(Y^{(i)} \mid X). \tag{44}$$

Then

$$p_{x|y^{(1)},y^{(2)},\ldots,y^{(r)}}(X \mid Y^{(1)},Y^{(2)},\ldots,Y^{(r)}) = \frac{p_{y^{(r)}|x}(Y^{(r)} \mid X)p_{x|y^{(1)},y^{(2)},\ldots,y^{(r-1)}}(X \mid Y^{(1)},Y^{(2)},\ldots,Y^{(r-1)})}{\int_{-\infty}^{+\infty} p_{y^{(r)}|x}(Y^{(r)} \mid X)p_{x|y^{(1)},y^{(2)},\ldots,y^{(r-1)}}(X \mid Y^{(1)},Y^{(2)},\ldots,Y^{(r-1)})dX}. \tag{45}$$

In addition, let x, $z^{(1)}$, $z^{(2)},\ldots,z^{(r)}$, $y^{(1)}$, $y^{(2)},\ldots,y^{(r)}$ be random vectors satisfying

$$p_{z^{(1)},z^{(2)},\ldots,z^{(r)}|x}(Z^{(1)},Z^{(2)},\ldots,Z^{(r)} \mid X) = \prod_{i=1}^{r} p_{z^{(i)}|x}(Z^{(i)} \mid X) \tag{46a}$$

$$p_{y^{(1)},y^{(2)},\ldots,y^{(r)}|x,z^{(1)},z^{(2)},\ldots,z^{(r)}}(Y^{(1)},Y^{(2)},\ldots,Y^{(r)} \mid X,Z^{(1)},Z^{(2)},\ldots,Z^{(r)}) = \prod_{i=1}^{r} p_{y^{(i)}|x,z^{(i)}}(Y^{(i)} \mid X,Z^{(i)}). \tag{46b}$$

Then

$$p_{z^{(r)}|x,y^{(1)},\ldots,y^{(r-1)}}(Z^{(r)} \mid X,Y^{(1)},\ldots,Y^{(r-1)}) = p_{z^{(r)}|x}(Z^{(r)} \mid X) \tag{47}$$

and

$$p_{x,z^{(r)}|y^{(1)},y^{(2)},\ldots,y^{(r)}}(X,Z^{(r)} \mid Y^{(1)},Y^{(2)},\ldots,Y^{(r)}) = \frac{p_{y^{(r)}|x,z^{(r)}}(Y^{(r)} \mid X,Z^{(r)})p_{z^{(r)}|x}(Z^{(r)} \mid X)p_{x|y^{(1)},\ldots,y^{(r-1)}}(X \mid Y^{(1)},\ldots,Y^{(r-1)})}{\int_{-\infty}^{+\infty} p_{y^{(r)}|x,z^{(r)}}(Y^{(r)} \mid X,Z^{(r)})p_{z^{(r)}|x}(Z^{(r)} \mid X)p_{x|y^{(1)},\ldots,y^{(r-1)}}(X \mid Y^{(1)},\ldots,Y^{(r-1)})dZ^{(r)}dX}. \tag{48}$$

PROOF The proof is deferred to Appendix C.

PROPOSITION 4 *Let $\{i_1,i_2,\ldots,i_r\} \subseteq \{1,2,\ldots,m\}$ be a set of indices such that $i_j \neq i_k$ for $j \neq k$. Then*

$$p_{x_{k+1},b_{k+1}^{(i_r)},\gamma_{k+1}^{(i_r)}|y_{k+1}^{(i_1)},\ldots,y_{k+1}^{(i_{r-1})},\mathcal{Y}_k}(X_{k+1},B_{k+1}^{(i_r)},\Gamma_{k+1}^{(i_r)} \mid Y_{k+1}^{(i_1)},\ldots,Y_{k+1}^{(i_{r-1})},\Upsilon_k) = p_{b_{k+1}^{(i_r)},\gamma_{k+1}^{(i_r)}|x_{k+1},\mathcal{Y}_k}(B_{k+1}^{(i_r)},\Gamma_{k+1}^{(i_r)} \mid X_{k+1},\Upsilon_k) \times p_{x_{k+1}|y_{k+1}^{(i_1)},\ldots,y_{k+1}^{(i_{r-1})},\mathcal{Y}_k}(X_{k+1} \mid Y_{k+1}^{(i_1)},\ldots,Y_{k+1}^{(i_{r-1})},\Upsilon_k). \tag{49}$$

PROOF This result follows immediately from Proposition 3.

Using Propositions 3 and 4, the following measurement update procedure can be constructed for every index $i \in \{1,2,\ldots,m\}$. Let $\{i_1,i_2,\ldots,i_m\}$ be an index sequence with $i_m = i$. Then the measurement update can be performed sequentially in the following order:

$$\begin{aligned} x_{k+1} \mid \mathcal{Y}_k &\rightarrow x_{k+1} \mid y_{k+1}^{(i_1)},\mathcal{Y}_k \\ &\rightarrow x_{k+1} \mid y_{k+1}^{(i_1)},y_{k+1}^{(i_2)},\mathcal{Y}_k \rightarrow \cdots \\ &\rightarrow x_{k+1} \mid y_{k+1}^{(i_1)},\ldots,y_{k+1}^{(i_{m-1})},\mathcal{Y}_k \\ &\rightarrow \begin{cases} x_{k+1} \mid \mathcal{Y}_{k+1} \\ \gamma_{k+1}^{(i)} \mid \mathcal{Y}_{k+1} \\ b_{k+1}^{(i)} \mid x_{k+1},\gamma_{k+1}^{(i)},\mathcal{Y}_{k+1} \end{cases} \end{aligned} \tag{50}$$

where each of the scalar measurement updates can be performed as follows.

Suppose that $x_{k+1} \mid y_{k+1}^{(i_1)},\ldots,y_{k+1}^{(i_{r-1})},\mathcal{Y}_k$ has been already computed. Then

1) Using the distributions $x_{k+1} \mid y_{k+1}^{(i_1)},\ldots,y_{k+1}^{(i_{r-1})},\mathcal{Y}_k$ and $b_{k+1}^{(i_r)},\gamma_{k+1}^{(i_r)} \mid x_{k+1},\mathcal{Y}_k$, construct the joint distribution $x_{k+1},b_{k+1}^{(i_r)},\gamma_{k+1}^{(i_r)} \mid y_{k+1}^{(i_1)},\ldots,y_{k+1}^{(i_{r-1})},\mathcal{Y}_k$, assuming that all the associated pdfs are Gaussian.

2) Perform a single measurement update

$$x_{k+1},b_{k+1}^{(i_r)},\gamma_{k+1}^{(i_r)} \mid y_{k+1}^{(i_1)},\ldots,y_{k+1}^{(i_{r-1})},\mathcal{Y}_k \rightarrow x_{k+1},b_{k+1}^{(i_r)},\gamma_{k+1}^{(i_r)} \mid y_{k+1}^{(i_1)},\ldots,y_{k+1}^{(i_r)},\mathcal{Y}_k \tag{51}$$

using the standard IMM measurement update procedure. Notice that the state vector is now $[x_{k+1}^T \;\; b_{k+1}^{(i_r)}]^T \in \mathbb{R}^{n+1}$, and there are only two modes: $\gamma_{k+1}^{(i_r)} = 0$ and $\gamma_{k+1}^{(i_r)} = 1$.

3) Using $x_{k+1},b_{k+1}^{(i_r)},\gamma_{k+1}^{(i_r)} \mid y_{k+1}^{(i_1)},\ldots,y_{k+1}^{(i_r)},\mathcal{Y}_k$, compute the marginal distribution $x_{k+1} \mid y_{k+1}^{(i_1)},\ldots,y_{k+1}^{(i_r)},\mathcal{Y}_k$ and, if $r = m$, the conditional distribution $b_{k+1}^{(i_r)},\gamma_{k+1}^{(i_r)} \mid x_{k+1},y_{k+1}^{(i_1)},\ldots,y_{k+1}^{(i_r)},\mathcal{Y}_k$, assuming, again, that all associated pdfs are Gaussian.

Using this procedure in a straightforward manner requires m^2 IMM scalar measurement update steps.

However, saving some miscellaneous results, this number of measurement updates can be reduced to $(m^2+3m-2)/2$. The resulting measurement update procedure is summarized in Section IVC as part of the entire estimation algorithm.

C. Algorithm Summary

At the beginning of the recursion cycle at time k, the quantities $\hat{x}_{k|k}$, $\hat{P}_{k|k}$, $\hat{\gamma}^{(i)}_{k|k}$, $\alpha^{(i)}_{k|k,k,k}(\xi)$, $\beta^{(i)}_{k|k,k,k}(\xi)$ and $\rho^{(i)}_{k|k,k,k}(\xi)$ for $i\in\{1,\dots,m\}$, $\xi\in\{0,1\}$ are available from the previous cycles.

1) Main state evolution: $x_k \mid \mathcal{Y}_k \Rightarrow x_{k+1} \mid \mathcal{Y}_k$.

$$\hat{x}_{k+1|k} = \Phi\hat{x}_{k|k} + \Psi u_{k+1} \tag{52a}$$

$$\hat{P}_{k+1|k} = \Phi\hat{P}_{k|k}\Phi^T + GQG^T. \tag{52b}$$

2) Fault probabilities time evolution: $\gamma^{(i)}_k \mid \mathcal{Y}_k \Rightarrow \gamma^{(i)}_{k+1} \mid \mathcal{Y}_k$. For every channel $i=1,2,\dots,m$:

$$\hat{\gamma}^{(i)}_{k+1|k} = P^{(i)}_{10}(1-\hat{\gamma}^{(i)}_{k|k}) + P^{(i)}_{11}\hat{\gamma}^{(i)}_{k|k}. \tag{53}$$

3) Measurement error state mixing due to fault probabilities evolution:
$b^{(i)}_k \mid \gamma^{(i)}_k, x_k, \mathcal{Y}_k \Rightarrow b^{(i)}_k \mid \gamma^{(i)}_{k+1}, x_k, \mathcal{Y}_k$. For every channel $i=1,2,\dots,m$ and $\xi\in\{0,1\}$:

$$\mu_{\xi\eta} = \frac{P^{(i)}_{\xi\eta}}{\xi\hat{\gamma}^{(i)}_{k+1|k} + (1-\xi)(1-\hat{\gamma}^{(i)}_{k+1|k})} \times (\eta\hat{\gamma}^{(i)}_{k|k} + (1-\eta)(1-\hat{\gamma}^{(i)}_{k|k})), \quad \eta\in\{0,1\} \tag{54a}$$

$$\alpha^{(i)}_{k|k+1,k,k}(\xi) = \sum_{\eta=0}^{1}\mu_{\xi\eta}\alpha^{(i)}_{k|k,k,k}(\eta) \tag{54b}$$

$$\beta^{(i)}_{k|k+1,k,k}(\xi) = \sum_{\eta=0}^{1}\mu_{\xi\eta}\beta^{(i)}_{k|k,k,k}(\eta) \tag{54c}$$

$$\rho^{(i)}_{k|k+1,k,k}(\xi) = \sum_{\eta=0}^{1}\mu_{\xi\eta}[\rho^{(i)}_{k|k,k,k}(\eta) + (\alpha^{(i)}_{k|k,k,k}(\eta) - \alpha^{(i)}_{k|k+1,k,k}(\xi))^2 + (\beta^{(i)}_{k|k,k,k}(\eta) - \beta^{(i)}_{k|k+1,k,k}(\xi))^T\hat{P}_{k|k} \times (\beta^{(i)}_{k|k,k,k}(\eta) - \beta^{(i)}_{k|k+1,k,k}(\xi))]. \tag{54d}$$

4) Measurement error state evolution: $b^{(i)}_k \mid \gamma^{(i)}_{k+1}, x_k, \mathcal{Y}_k \Rightarrow b^{(i)}_{k+1} \mid \gamma^{(i)}_{k+1}, x_k, \mathcal{Y}_k$. For every channel $i=1,2,\dots,m$ and $\xi\in\{0,1\}$:

$$\alpha^{(i)}_{k+1|k+1,k,k}(\xi) = a^{(i)}(\xi)\alpha^{(i)}_{k|k+1,k,k}(\xi) \tag{55a}$$

$$\beta^{(i)}_{k+1|k+1,k,k}(\xi) = a^{(i)}(\xi)\beta^{(i)}_{k|k+1,k,k}(\xi) \tag{55b}$$

$$\rho^{(i)}_{k+1|k+1,k,k}(\xi) = {a^{(i)}}^2(\xi)\rho^{(i)}_{k|k+1,k,k}(\xi) + {g^{(i)}}^2(\xi)q^{(i)}(\xi). \tag{55c}$$

5) Measurement error mixing due to the main state evolution: $b^{(i)}_{k+1} \mid \gamma^{(i)}_{k+1}, x_k, \mathcal{Y}_k \Rightarrow b^{(i)}_{k+1} \mid \gamma^{(i)}_{k+1}, x_{k+1}, \mathcal{Y}_k$. For every channel $i=1,2,\dots,m$ and $\xi\in\{0,1\}$:

$$\alpha^{(i)}_{k+1|k+1,k+1,k}(\xi) = \alpha^{(i)}_{k+1|k+1,k,k}(\xi) \tag{56a}$$

$$\beta^{(i)}_{k+1|k+1,k+1,k}(\xi) = \hat{P}^{-1}_{k+1|k}\Phi\hat{P}_{k|k}\beta^{(i)}_{k+1|k+1,k,k}(\xi) \tag{56b}$$

$$\rho^{(i)}_{k+1|k+1,k+1,k}(\xi) = \rho^{(i)}_{k+1|k+1,k,k}(\xi) + {\beta^{(i)}_{k+1|k+1,k,k}}^T(\xi) \times \hat{P}_{k|k}\beta^{(i)}_{k+1|k+1,k,k}(\xi) - {\beta^{(i)}_{k+1|k+1,k+1,k}}^T(\xi) \times \hat{P}_{k+1|k}\beta^{(i)}_{k+1|k+1,k+1,k}(\xi). \tag{56c}$$

6) Measurement update:

$$x_{k+1} \mid \mathcal{Y}_k \Rightarrow x_{k+1} \mid \mathcal{Y}_{k+1}$$

$$\gamma^{(i)}_{k+1} \mid \mathcal{Y}_k \Rightarrow \gamma^{(i)}_{k+1} \mid \mathcal{Y}_{k+1}$$

$$b^{(i)}_{k+1} \mid \gamma^{(i)}_{k+1}, x_{k+1}, \mathcal{Y}_k \Rightarrow b^{(i)}_{k+1} \mid \gamma^{(i)}_{k+1}, x_{k+1}, \mathcal{Y}_{k+1}.$$

Perform the following sequence of $(m-1)$ scalar measurement updates:

$$\begin{aligned} x_{k+1} \mid \mathcal{Y}_k &\rightarrow x_{k+1} \mid y^{(1)}_{k+1}, \mathcal{Y}_k \\ &\rightarrow x_{k+1} \mid y^{(1)}_{k+1}, y^{(2)}_{k+1}, \mathcal{Y}_k \rightarrow \cdots \\ &\rightarrow x_{k+1} \mid y^{(1)}_{k+1}, \dots, y^{(m-1)}_{k+1}, \mathcal{Y}_k. \end{aligned} \tag{57}$$

Each scalar measurement update step comprises the following parts. Let

$$x_{k+1} \mid y^{(i_1)}_{k+1}, \dots, y^{(i_{r-1})}_{k+1}, \mathcal{Y}_k \sim \mathcal{N}(\hat{x}^{(i_{r-1})}, \hat{P}^{(i_{r-1})}) \tag{58}$$

and denote, for simplicity,

$$\alpha_\xi \triangleq \alpha^{(i)}_{k+1|k+1,k+1,k}(\xi) \tag{59a}$$

$$\beta_\xi \triangleq \beta^{(i)}_{k+1|k+1,k+1,k}(\xi) \tag{59b}$$

$$\rho_\xi \triangleq \rho^{(i)}_{k+1|k+1,k+1,k}(\xi) \tag{59c}$$

$$p_\xi \triangleq \Pr\{\gamma^{(i)}_{k+1} = \xi \mid \mathcal{Y}_k\}. \tag{59d}$$

Then

a) Construct the joint distribution $x_{k+1}, b^{(i_r)}_{k+1}, \gamma^{(i_r)}_{k+1} \mid y^{(i_1)}_{k+1}, \dots, y^{(i_{r-1})}_{k+1}, \mathcal{Y}_k$. For $\xi\in\{0,1\}$

$$\Pr\{\gamma^{(i)}_{k+1} = \xi \mid y^{(i_1)}_{k+1}, \dots, y^{(i_{r-1})}_{k+1}, \mathcal{Y}_k\} = p_\xi \tag{60a}$$

$$x_{k+1}, b^{(i_r)}_{k+1} \mid \gamma^{(i_r)}_{k+1} = \xi, y^{(i_1)}_{k+1}, \dots, y^{(i_{r-1})}_{k+1}, \mathcal{Y}_k \sim \mathcal{N}(\hat{z}^{(i_{r-1})}(\xi), M^{(i_{r-1})}(\xi)) \tag{60b}$$

where

$$\hat{z}^{(i_{r-1})}(\xi) = \begin{bmatrix} \hat{x}^{(i_{r-1})} \\ \alpha_\xi \end{bmatrix} \tag{61a}$$

$$M^{(i_{r-1})}(\xi)=\begin{bmatrix}\hat{P}^{(i_{r-1})} & \hat{P}^{(i_{r-1})}\beta_\xi\\ \beta_\xi^T\hat{P}^{(i_{r-1})} & \rho_\xi+\beta_\xi^T\hat{P}^{(i_{r-1})}\beta_\xi\end{bmatrix}. \quad (61b)$$

b) Perform a single measurement update:

$$\Pr\{\gamma_{k+1}^{(i)}=\xi \mid y_{k+1}^{(i_1)},\ldots,y_{k+1}^{(i_r)},\mathcal{Y}_k\}=p_\xi^{(i_r)},\quad \xi\in\{0,1\} \quad (62a)$$

$$x_{k+1},b_{k+1}^{(i_r)} \mid \gamma_{k+1}^{(i_r)}=\xi,y_{k+1}^{(i_1)},\ldots,y_{k+1}^{(i_r)},\mathcal{Y}_k\sim\mathcal{N}(\hat{z}^{(i_r)}(\xi),M^{(i_r)}(\xi)),\quad \xi\in\{0,1\} \quad (62b)$$

where $p_\xi^{(i_r)}$, $\hat{z}^{(i_r)}(\xi)$, and $M^{(i_r)}(\xi)$ are computed as

$$\tilde{y}_{k+1}^{(i_r)}(\xi)=y_{k+1}^{(i_r)}-[h_k^{(i)T}\ \ c_k^{(i)}(\xi)]\hat{z}^{(i_{r-1})}(\xi) \quad (63a)$$

$$\sigma_{\tilde{y}}^2(\xi)=[h_k^{(i)T}\ \ c_k^{(i)}(\xi)]M^{(i_{r-1})}(\xi)\begin{bmatrix}h_k^{(i)}\\ c_k^{(i)}(\xi)\end{bmatrix}+R^{(i)} \quad (63b)$$

$$K(\xi)=M^{(i_{r-1})}(\xi)\begin{bmatrix}h_k^{(i)}\\ c_k^{(i)}(\xi)\end{bmatrix}\frac{1}{\sigma_{\tilde{y}}^2(\xi)} \quad (63c)$$

$$\hat{z}^{(i_r)}(\xi)=\hat{z}^{(i_{r-1})}(\xi)+K(\xi)\tilde{y}_{k+1}^{(i_r)}(\xi) \quad (63d)$$

$$(I-KH)(\xi)=I-K(\xi)[h_k^{(i)T}\ \ c_k^{(i)}(\xi)] \quad (63e)$$

$$M^{(i_r)}(\xi)=(I-KH)(\xi)M^{(i_{r-1})}(\xi)(I-KH)^T(\xi)+K(\xi)R^{(i)}K^T(\xi) \quad (63f)$$

$$f_\xi=\frac{1}{\sqrt{\sigma_{\tilde{y}}^2(\xi)}}\exp\left[-\frac{(\tilde{y}_{k+1}^{(i_r)}(\xi))^2}{2\sigma_{\tilde{y}}^2(\xi)}\right] \quad (63g)$$

and

$$p_\xi^{(i_r)}=\frac{f_\xi p_\xi}{f_0p_0+f_1p_1}. \quad (64)$$

c) Compute the marginal distribution $x_{k+1} \mid y_{k+1}^{(i_1)},\ldots,y_{k+1}^{(i_r)},\mathcal{Y}_k$. Let $\hat{z}^{(i_r)}(\xi)$ and $M^{(i_r)}(\xi)$ be partitioned as

$$\hat{z}^{(i_r)}(\xi)=\begin{bmatrix}\hat{z}_x(\xi)\\ \hat{z}_b(\xi)\end{bmatrix},\qquad \hat{z}_x(\xi)\in\mathbb{R}^n \quad (65a)$$

$$M^{(i_r)}(\xi)=\begin{bmatrix}M_{xx}(\xi) & m_{xb}(\xi)\\ m_{xb}^T(\xi) & m_{bb}(\xi)\end{bmatrix},\qquad M_{xx}(\xi)\in\mathbb{R}^{n\times n}. \quad (65b)$$

Then

$$\hat{x}^{(i_r)}=\hat{z}_x(0)p_0^{(i_r)}+\hat{z}_x(1)p_1^{(i_r)} \quad (66a)$$

$$\hat{P}^{(i_r)}=\sum_{\xi=0}^{1}p_\xi^{(i_r)}[M_{xx}(\xi)+(\hat{z}_x(\xi)-\hat{x}^{(i_r)})(\hat{z}_x(\xi)-\hat{x}^{(i_r)})^T]. \quad (66b)$$

After each measurement update save the resulting mean and covariance of the main state x_{k+1}, given by (66a) and (66b), respectively. Then, for each index i in the set $\{m,m-1,\ldots,1\}$, perform the following measurement update sequence similarly to (57):

$$\begin{aligned}x_{k+1} \mid y_{k+1}^{(1)},\ldots,y_{k+1}^{(i-1)},\mathcal{Y}_k &\\ \rightarrow\ & x_{k+1} \mid y_{k+1}^{(1)},\ldots,y_{k+1}^{(i-1)},y_{k+1}^{(m)},\mathcal{Y}_k\\ \rightarrow\ & x_{k+1} \mid y_{k+1}^{(1)},\ldots,y_{k+1}^{(i-1)},y_{k+1}^{(m)},y_{k+1}^{(m-1)},\mathcal{Y}_k \ \rightarrow\ \cdots\\ \rightarrow\ & x_{k+1} \mid y_{k+1}^{(1)},\ldots,y_{k+1}^{(i-1)},y_{k+1}^{(m)},\ldots,y_{k+1}^{(i+1)},\mathcal{Y}_k\\ \rightarrow\ & \begin{cases}x_{k+1} \mid \mathcal{Y}_{k+1}\\ \gamma_{k+1}^{(i)} \mid \mathcal{Y}_{k+1}\\ b_{k+1}^{(i)} \mid x_{k+1},\gamma_{k+1}^{(i)},\mathcal{Y}_{k+1}\end{cases}.\end{aligned} \quad (67)$$

Notice that after the last measurement update, which is done using $y_{k+1}^{(i)}$, the parameters of both the marginal distribution of $x_{k+1} \mid \mathcal{Y}_{k+1}$ and the conditional distribution of $b_{k+1}^{(i)},\gamma_{k+1}^{(i)} \mid x_{k+1},\mathcal{Y}_{k+1}$ must be computed. This is done in the following manner:

$$\hat{x}_{k+1|k+1}^{(i)}=\hat{x}^{(i)} \quad (68a)$$

$$\hat{P}_{k+1|k+1}^{(i)}=\hat{P}^{(i)} \quad (68b)$$

$$\alpha_{k+1|k+1,k+1,k+1}^{(i)}(\xi)=\hat{z}_b(\xi) \quad (68c)$$

$$\beta_{k+1|k+1,k+1,k+1}^{(i)}(\xi)=M_{xx}(\xi)^{-1}m_{xb}(\xi) \quad (68d)$$

$$\rho_{k+1|k+1,k+1,k+1}^{(i)}(\xi)=m_{bb}(\xi)-\beta_{k+1|k+1,k+1,k+1}^{(i)\,T}(\xi)\times M_{xx}(\xi)\beta_{k+1|k+1,k+1,k+1}^{(i)}(\xi) \quad (68e)$$

$$\hat{\gamma}_{k+1|k+1}^{(i)}=p_1^{(i)}. \quad (68f)$$

As a result of this measurement update procedure the m pairs of parameters $(\hat{x}_{k+1|k+1}^{(i)},\hat{P}_{k+1|k+1}^{(i)})$ are obtained. These parameters are then averaged to yield a more accurate estimate of the main state x_{k+1}:

$$\hat{x}_{k+1|k+1}=\frac{1}{m}\sum_{i=1}^{m}\hat{x}_{k+1|k+1}^{(i)} \quad (69a)$$

$$\hat{P}_{k+1|k+1}=\frac{1}{m}\sum_{i=1}^{m}\hat{P}_{k+1|k+1}^{(i)}. \quad (69b)$$

REMARK 2 Although the new algorithm has been derived for systems where all measurement channels are fault prone, it is also suitable for systems where some measurements can be assumed to be free of faults. The only change in this case is that Step 6 of the proposed algorithm must be preceded by the measurement update of the main state using the fault-free measurements.

The computational complexity of the proposed algorithm is analyzed in the next section, where it is also compared with that of the ordinary IMM filter.

TABLE I
Computational Load per Cycle (FLOP Count) of Proposed Algorithm

Step	Multiplication, Division	Addition, Subtraction	$n \times n$ Matrix Inversion	Exponentiation, Square Root	Times
1	$\frac{3}{2}n^2(n+1)$	$(n^2/2)(3n+1)$	0	0	1
2	$2m$	$2m$	0	0	1
3	$4(n^2+2n+4)m$	$2(n^2+3n+7)m$	0	0	1
4	$2(n+2)m$	$2m$	0	0	1
5	$4n(2n+1)m$	$4n(2n-1)m$	1	0	1
6.1	n^2+n	n^2-1	0	0	$(m^2+3m-2)/2$
6.2	$3n^3+15n^2+32n+33$	$3n^3+10n^2+17n+12$	0	2	$(m^2+3m-2)/2$
6.3:					
$x \mid \mathcal{Y}$	$2n(n+2)$	$\frac{3}{2}n(n+3)$	0	0	$(m^2+3m-2)/2$
$b,\gamma \mid x,\mathcal{Y}$	$n(n+1)$	n^2-1	1	0	$2m$
Averaging	$(n(n+3))/2$	$((n(n+3))/2)(m-1)$	0	0	1

TABLE II
Computational Load per Cycle (FLOP Count) of Ordinary IMM Algorithm

Step	Multiplication, Division	Addition, Subtraction	Exponentiation, Square Root	Times
Mode evolution	$S(S-1)$	$S(S-1)$	0	1
Mixing	$S^2(N^2+2N+2)$	$S(2S-1)N(N+3)/2$	0	1
State evolution	$\frac{3}{2}n^2(n+1)+m(n^2+N+1)$	$((n(n+1))/2)(3n-2)+n+m(n^2-n+1)$	0	S
State update	$\frac{3}{2}N^3+3N^2+\frac{11}{2}N+1$	$\frac{3}{2}N^3+N^2/2+3N$	0	Sm
Mode update	$S(5m+1)$	$S-1$	$2Sm$	1
x_k estimate	Sn	$(S-1)n$	0	1

TABLE III
Computational Burden Comparison (FLOP Count) of Proposed Algorithm versus Ordinary IMM Algorithm for $n = 4$

m	New	IMM	IMM/New
1	2257	1829	0.8
2	6491	9455	1.5
3	11877	41635	3.5
4	18415	166907	9.1
5	26105	636635	24.3
6	34947	2388155	68.3
7	44941	9035387	201.1

V. COMPLEXITY ANALYSIS

Table I presents the number of floating point operations (FLOPs) per cycle in the proposed algorithm. The analysis is based on the following set of assumptions.

Assumption 4 Only the upper triangle is computed in any symmetric matrix.

Assumption 5 Expressions like GQG^T, $a^{(i)}(\xi)^2$ or $g^{(i)}(\xi)^2 q^{(i)}(\xi)$ are computed off-line.

Assumption 6 Only the main state estimate is required as the algorithm's output.

To demonstrate the computational efficiency of the proposed algorithm a complexity analysis of the ordinary IMM was also carried out. The analysis is also based on the set of Assumptions 4–6. The results are summarized in Table II, where S denotes the number of possible modes (in the case under consideration $S = 2^m$) and N denotes the total state dimension ($N = n + m$).

Table I shows that when the number of measurements is sufficiently large, the computational complexity of the proposed algorithm is $O(n^3m^2)$. The computational complexity of the ordinary IMM algorithm, on the other hand, is $O(2^{2m}m^2)$. In other words, the number of FLOPs in the new algorithm is polynomial in the number of measurement channels, whereas in the IMM algorithm this relation is exponential.

Finally, Table III presents a numerical comparison of the complexities of both algorithms for 4 main states ($n = 4$). It is assumed that the execution of all FLOP types takes the same time, and that matrix inversions are performed using the UDU^T decomposition. Table III shows that, starting from $m = 2$, the proposed algorithm exhibits a clear advantage over the ordinary IMM.

VI. SIMULATION STUDY

A numerical simulation study has been carried out to demonstrate that the proposed algorithm exhibits similar estimation performance to that of the standard IMM filter, while incurring only a small fraction of the associated computational cost. As an example, a spacecraft attitude estimation problem is addressed.

Consider a spacecraft in a circular orbit around Earth. The spacecraft performs a torque-free angular motion relative to some reference coordinate system. The spacecraft attitude is represented by three Euler angles: yaw, pitch, and roll. A momentum wheel is installed along the pitch axis. Denote the wheel momentum by h_w. The spacecraft body axes are fixed along its principal axes. Let I_{xx}, I_{yy}, and I_{zz} be the spacecraft principal moments of inertia.

It is assumed that the Euler angles are sufficiently small so that the pitch and roll-yaw dynamics are uncoupled and, consequently, can be treated separately. Only the roll-yaw dynamics is considered herein. The linearized equations of the spacecraft roll-yaw angular motion are [14, pp. 108, 251]

$$\dot{\varphi} = \omega_x \tag{70a}$$

$$\dot{\psi} = \omega_z \tag{70b}$$

$$\dot{\omega}_x = \frac{h_w\omega_0}{I_{xx}}\varphi + \frac{h_w}{I_{xx}}\omega_z + n_x \tag{70c}$$

$$\dot{\omega}_z = \frac{h_w\omega_0}{I_{zz}}\psi - \frac{h_w}{I_{zz}}\omega_x + n_z \tag{70d}$$

where φ and ψ are the roll and yaw angles, respectively, ω_x, ω_z are the spacecraft angular rate components, ω_0 is the satellite circular frequency of its Earth orbit and n_x, n_z are the specific torque noise components. The process noises n_x and n_z are mutually independent zero-mean Gaussian white processes with power spectral density (PSD) σ_n^2. The initial values of the states φ, ψ, ω_x, and ω_z are independent zero-mean Gaussian random variables with

$$\text{var}[\varphi(0)] = \text{var}[\psi(0)] = 10^2 \text{ deg}^2 \tag{71a}$$

$$\text{var}[\omega_x(0)] = \text{var}[\omega_z(0)] = 1^2 \text{ deg}^2/\text{s}^2. \tag{71b}$$

Five independent sensors are installed onboard the satellite: two horizon sensors, measuring the roll angle and described by

$$y^{(i)} = \varphi + \gamma^{(i)}b^{(i)} + v^{(i)}, \qquad i \in \{1,2\}, \quad v^{(i)} \sim \mathcal{N}(0,\sigma_{\text{vh}}^2) \tag{72}$$

and three rate gyros installed along 3 different directions in the x-z plane:

$$\begin{bmatrix} y^{(3)} \\ y^{(4)} \\ y^{(5)} \end{bmatrix} = \begin{bmatrix} \sqrt{3}/2 & -1/2 \\ 0 & 1 \\ -\sqrt{3}/2 & -1/2 \end{bmatrix} \begin{bmatrix} \omega_x \\ \omega_z \end{bmatrix} + \begin{bmatrix} \gamma^{(3)}b^{(3)} \\ \gamma^{(4)}b^{(4)} \\ \gamma^{(5)}b^{(5)} \end{bmatrix} + \begin{bmatrix} v^{(3)} \\ v^{(4)} \\ v^{(5)} \end{bmatrix}, \qquad v^{(i)} \sim \mathcal{N}(0,\sigma_{\text{vg}}^2). \tag{73}$$

The measurements are acquired by these sensors at a rate of 1 Hz, and the continuous-time system (70) is discretized in time accordingly. All measurement channels are prone to faults that take the form of biases changing their values each time they appear. In other words, the sensor faulty dynamics can be described by

$$b_{k+1}^{(i)} = \gamma_{k+1}^{(i)}b_k^{(i)} + [(1-\gamma_{k+1}^{(i)})k_b\sigma_{\text{vh}} + \gamma_{k+1}^{(i)}\sigma_{\text{wh}}]\tilde{w}_{k+1}^{(i)}, \qquad i \in \{1,2\} \tag{74a}$$

$$b_{k+1}^{(i)} = \gamma_{k+1}^{(i)}b_k^{(i)} + [(1-\gamma_{k+1}^{(i)})k_b\sigma_{\text{vg}} + \gamma_{k+1}^{(i)}\sigma_{\text{wg}}]\tilde{w}_{k+1}^{(i)}, \qquad i \in \{3,4,5\} \tag{74b}$$

where $\tilde{w}_{k+1}^{(i)} \sim \mathcal{N}(0,1)$ is the measurement bias process noise and k_b is bias/measurement noise standard deviation ratio. The spacecraft parameter values are summarized in Table IV.

TABLE IV
Spacecraft Parameters

Parameter	Value
ω_0	1.1×10^{-3} rad/sec
I_{xx}	15 kg-m^2
I_{zz}	20 kg-m^2
h_w	20 kg-m^2/sec
σ_n	7.6×10^{-3} deg/sec$^{3/2}$
σ_{vh}	1 deg
σ_{vg}	0.1 deg/sec
$P_{11}^{(i)}$	0.995
$P_{10}^{(i)}$	0.02
σ_{wh}	10^{-5} rad
σ_{wg}	10^{-5} rad/sec

A statistical Monte-Carlo investigation is performed to compare the proposed algorithm with the ordinary IMM algorithm. Both algorithms are run 2700 times, where the duration of each run is 1000 time steps. Figs. 1 and 2 present the rms state estimation errors for both algorithms, corresponding to a bias/measurement noise standard deviation ratio $k_b = 4.0$. In the case of measurement fault states the estimation errors are computed for the effective measurement errors $\gamma^{(i)}b^{(i)}$. It can be observed that the estimation errors of the Euler angles and the roll measurement biases are close in both algorithms, and the estimation errors of the angular velocities and their measurement biases are almost identical.

Fig. 3 presents the corresponding fault estimation rms errors for both algorithms. One can clearly see that both filters exhibit almost identical fault estimation performance.

In sum, the numerical simulation study demonstrates that, in this example, the estimation performance of the proposed algorithm closely approximates the performance of the standard IMM filter. At the same time, Table III shows that, for the problem addressed, the proposed algorithm's FLOP count is only about 4% of that associated with the

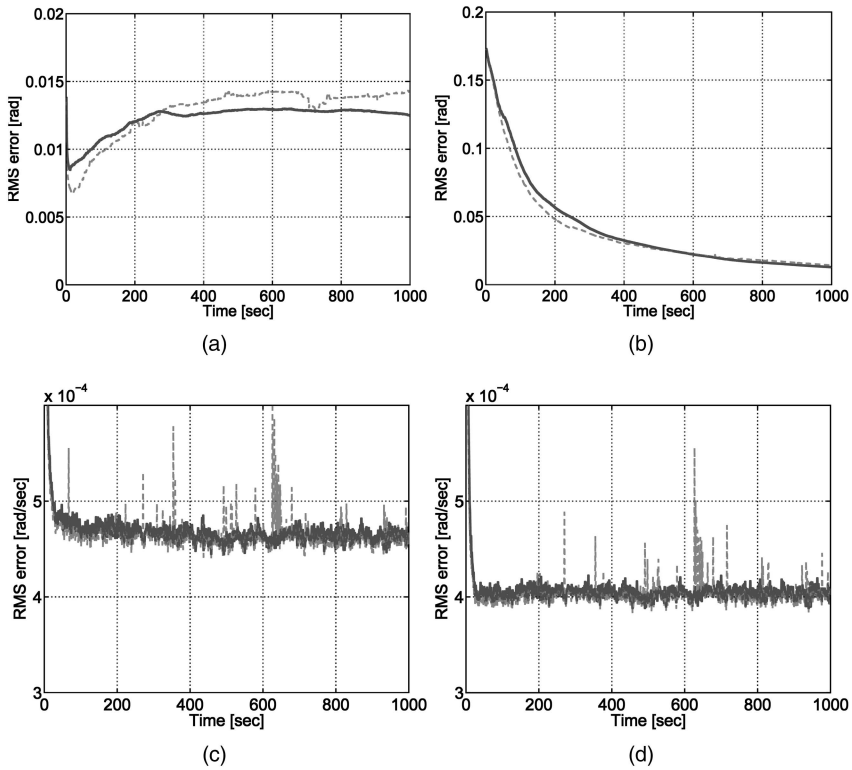

Fig. 1. Main state rms estimation errors for new algorithm (bold solid line) and IMM algorithm (thin dashed line). (a) φ. (b) ψ. (c) ω_x. (d) ω_z.

standard IMM filter. Therefore, it can be stated that the proposed algorithm is superior to the ordinary IMM filter in terms of computational efficiency. Of course, this conclusion holds only for systems satisfying the structural model assumptions specified in Section II.

VII. CONCLUSIONS

An IMM-based fault-tolerant estimation algorithm has been presented. The algorithm is tailored for systems characterized by a low process noise and independent fault-prone scalar measurement channels. This algorithm handles different measurement faults separately, thus reducing the overall computational burden. The computational complexity of the proposed algorithm has been shown to be polynomial in the number of fault-prone measurements, unlike the ordinary IMM algorithm, where it is exponential. In an example problem of spacecraft attitude estimation, it has been shown that the performance of the proposed algorithm closely approximates the performance of the ordinary IMM algorithm, while requiring only a modest fraction of the computational load.

Although the new algorithm has been derived for systems where all measurement channels are fault prone, it is straightforward to extend it to a wider class of systems, where some measurements are free of faults.

APPENDIX A. PROOF OF PROPOSITION 1

The proof is by mathematical induction. First, mutual independence of x_0 and the elements of γ_0 and b_0 yields

$$p_{x_0,b_0,\gamma_0}(X_0,B_0,\Gamma_0) = p_{x_0}(X_0)\prod_{i=1}^{m}[p_{b_0^{(i)}}(B_0^{(i)})\Pr\{\gamma_0^{(i)} = \Gamma_0^{(i)}\}] \tag{75}$$

which is (23a) for $k = 0$. Assume now that (23a) holds for some $k \geq 0$. Using the Chapman-Kolmogorov equation, (3) and (4) gives

$$\begin{aligned}
&p_{b_{k+1},\gamma_{k+1}|x_k,\mathcal{Y}_k}(B_{k+1},\Gamma_{k+1} \mid X_k,\Upsilon_k)\\
&\quad= \int_{-\infty}^{+\infty} p_{b_{k+1},\gamma_{k+1}|b_k,\gamma_k}(B_{k+1},\Gamma_{k+1} \mid B_k,\Gamma_k)\\
&\qquad p_{b_k,\gamma_k|x_k,\mathcal{Y}_k}(B_k,\Gamma_k \mid X_k,\Upsilon_k)dB_k d\Gamma_k\\
&\quad= \int_{-\infty}^{+\infty}\prod_{i=1}^{m}[p_{b_{k+1}^{(i)},\gamma_{k+1}^{(i)}|b_k^{(i)},\gamma_k^{(i)}}(B_{k+1}^{(i)},\Gamma_{k+1}^{(i)} \mid B_k^{(i)},\Gamma_k^{(i)})\\
&\qquad p_{b_k^{(i)},\gamma_k^{(i)}|x_k,\mathcal{Y}_k}(B_k^{(i)},\Gamma_k^{(i)} \mid X_k,\Upsilon_k)dB_k^{(i)}d\Gamma_k^{(i)}]\\
&\quad= \prod_{i=1}^{m}\left[\int_{-\infty}^{+\infty} p_{b_{k+1}^{(i)},\gamma_{k+1}^{(i)}|b_k^{(i)},\gamma_k^{(i)}}(B_{k+1}^{(i)},\Gamma_{k+1}^{(i)} \mid B_k^{(i)},\Gamma_k^{(i)})\right.\\
&\qquad\left. p_{b_k^{(i)},\gamma_k^{(i)}|x_k,\mathcal{Y}_k}(B_k^{(i)},\Gamma_k^{(i)} \mid X_k,\Upsilon_k)dB_k^{(i)}d\Gamma_k^{(i)}\right]\\
&\quad= \prod_{i=1}^{m} p_{b_{k+1}^{(i)},\gamma_{k+1}^{(i)}|x_k,\mathcal{Y}_k}(B_{k+1}^{(i)},\Gamma_{k+1}^{(i)} \mid X_k,\Upsilon_k)
\end{aligned} \tag{76}$$

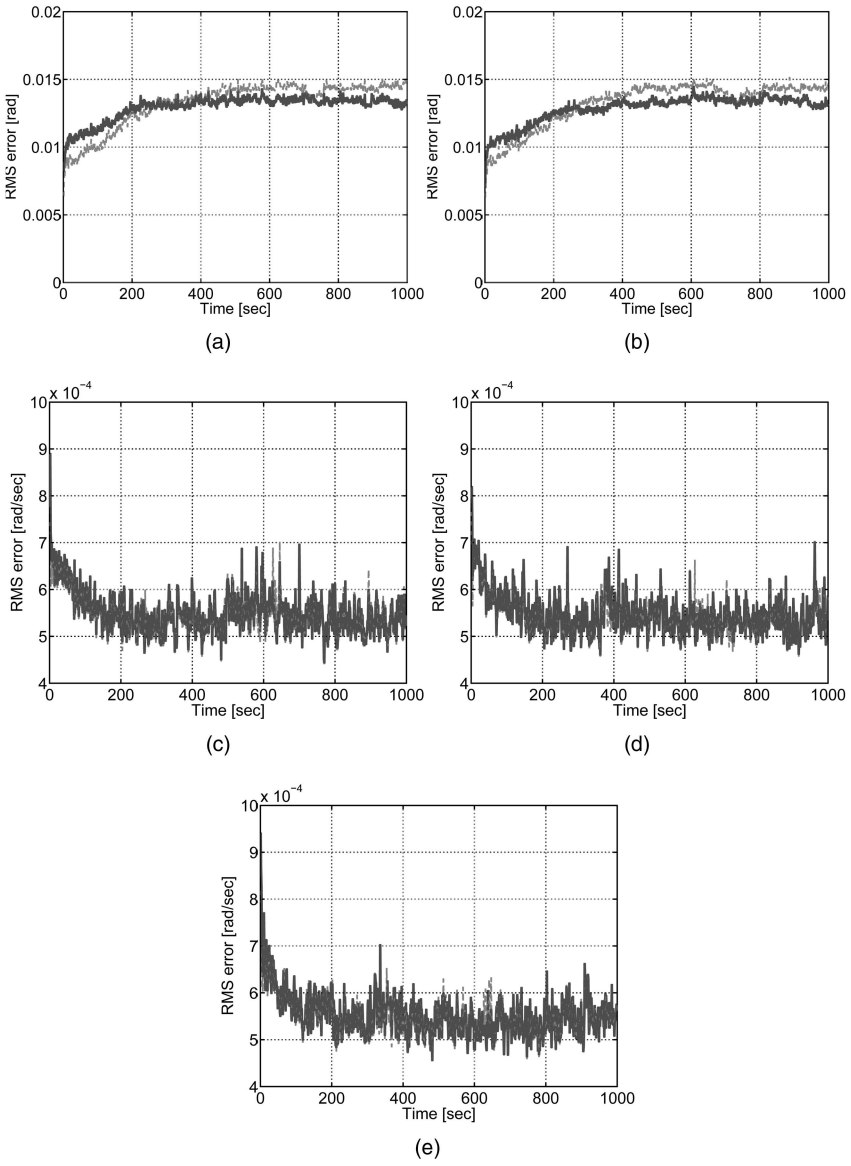

Fig. 2. Faulty state rms estimation errors for new algorithm (bold solid line) and IMM algorithm (thin dashed line). (a) $\gamma^{(1)}b^{(1)}$. (b) $\gamma^{(2)}b^{(2)}$. (c) $\gamma^{(3)}b^{(3)}$. (d) $\gamma^{(4)}b^{(4)}$. (e) $\gamma^{(5)}b^{(5)}$.

which yields (23b). Now, by the Markov property

$$\begin{aligned} &p_{b_{k+1},\gamma_{k+1}|x_{k+1},\mathcal{Y}_k}(B_{k+1},\Gamma_{k+1}\mid X_{k+1},\Upsilon_k)\\ &\quad=\int_{-\infty}^{+\infty} p_{b_{k+1},\gamma_{k+1}|x_k,\mathcal{Y}_k}(B_{k+1},\Gamma_{k+1}\mid X_k,\Upsilon_k)\\ &\qquad\times p_{x_k|x_{k+1},\mathcal{Y}_k}(X_k\mid X_{k+1},\Upsilon_k)dX_k\\ &\quad=\int_{-\infty}^{+\infty} p_{b_{k+1},\gamma_{k+1}|x_k,\mathcal{Y}_k}(B_{k+1},\Gamma_{k+1}\mid X_k,\Upsilon_k)\\ &\qquad\times\frac{p_{x_{k+1}|x_k}(X_{k+1}\mid X_k)}{p_{x_{k+1}|\mathcal{Y}_k}(X_{k+1}\mid\Upsilon_k)}p_{x_k|\mathcal{Y}_k}(X_k\mid\Upsilon_k)dX_k. \end{aligned} \tag{77}$$

But, due to Assumption 1

$$p_{x_{k+1}|x_k}(X_{k+1}\mid X_k)\approx\delta(X_{k+1}-\Phi X_k). \tag{78}$$

Substituting (78) into (77) and using (76) gives

$$\begin{aligned} &p_{b_{k+1},\gamma_{k+1}|x_{k+1},\mathcal{Y}_k}(B_{k+1},\Gamma_{k+1}\mid X_{k+1},\Upsilon_k)\\ &\quad\approx\int_{-\infty}^{+\infty} p_{b_{k+1},\gamma_{k+1}|x_k,\mathcal{Y}_k}(B_{k+1},\Gamma_{k+1}\mid X_k,\Upsilon_k)\\ &\qquad\times\frac{\delta(X_{k+1}-\Phi X_k)}{p_{x_{k+1}|\mathcal{Y}_k}(X_{k+1}\mid\Upsilon_k)}p_{x_k|\mathcal{Y}_k}(X_k\mid\Upsilon_k)dX_k\\ &\quad=p_{b_{k+1},\gamma_{k+1}|x_k,\mathcal{Y}_k}(B_{k+1},\Gamma_{k+1}\mid\Phi^{-1}X_{k+1},\Upsilon_k)\frac{p_{x_k|\mathcal{Y}_k}(\Phi^{-1}X_{k+1}\mid\Upsilon_k)}{p_{x_{k+1}|\mathcal{Y}_k}(X_{k+1}\mid\Upsilon_k)}\\ &\quad=\frac{p_{x_k|\mathcal{Y}_k}(\Phi^{-1}X_{k+1}\mid\Upsilon_k)}{p_{x_{k+1}|\mathcal{Y}_k}(X_{k+1}\mid\Upsilon_k)}\\ &\qquad\times\prod_{i=1}^{m}p_{b_{k+1}^{(i)},\gamma_{k+1}^{(i)}|x_k,\mathcal{Y}_k}(B_{k+1}^{(i)},\Gamma_{k+1}^{(i)}\mid\Phi^{-1}X_{k+1},\Upsilon_k)\\ &\quad=\prod_{i=1}^{m}p_{b_{k+1}^{(i)},\gamma_{k+1}^{(i)}|x_{k+1},\mathcal{Y}_k}(B_{k+1}^{(i)},\Gamma_{k+1}^{(i)}\mid X_{k+1},\Upsilon_k) \end{aligned} \tag{79}$$

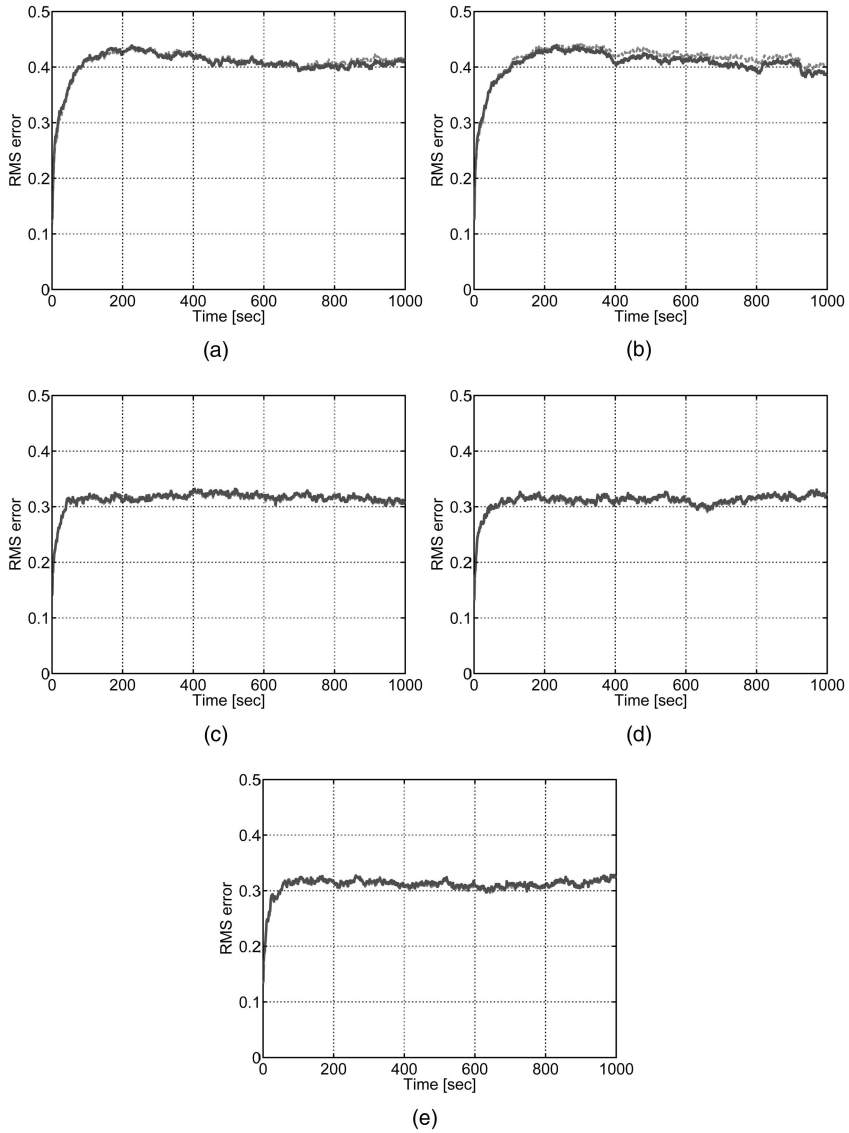

Fig. 3. Fault rms estimation errors for new algorithm (bold solid line) and IMM algorithm (thin dashed line). (a) $\gamma^{(1)}$. (b) $\gamma^{(2)}$. (c) $\gamma^{(3)}$. (d) $\gamma^{(4)}$. (e) $\gamma^{(5)}$.

which yields (23c). Finally, using Bayes' law gives

$$
\begin{aligned}
&p_{b_{k+1},\gamma_{k+1}|x_{k+1},\mathcal{Y}_{k+1}}(B_{k+1},\Gamma_{k+1} \mid X_{k+1},\Upsilon_{k+1}) \\
&\quad = \frac{p_{y_{k+1}|x_{k+1},b_{k+1},\gamma_{k+1}}(Y_{k+1} \mid X_{k+1},B_{k+1},\Gamma_{k+1})}{p_{y_{k+1}|x_{k+1}},\mathcal{Y}_k(Y_{k+1} \mid X_{k+1},\Upsilon_k)} p_{b_{k+1},\gamma_{k+1}|x_{k+1},\mathcal{Y}_k}(B_{k+1},\Gamma_{k+1} \mid X_{k+1},\Upsilon_k) \\
&\quad = \frac{\prod_{i=1}^{m}[p_{y_{k+1}^{(i)}|x_{k+1},b_{k+1}^{(i)},\gamma_{k+1}^{(i)}}(Y_{k+1}^{(i)} \mid X_{k+1},B_{k+1}^{(i)},\Gamma_{k+1}^{(i)}) p_{b_{k+1}^{(i)},\gamma_{k+1}^{(i)}|x_{k+1},\mathcal{Y}_k}(B_{k+1}^{(i)},\Gamma_{k+1}^{(i)} \mid X_{k+1},\Upsilon_k)]}{p_{y_{k+1}|x_{k+1}},\mathcal{Y}_k(Y_{k+1} \mid X_{k+1},\Upsilon_k)} \\
&\quad = \prod_{i=1}^{m} p_{b_{k+1}^{(i)},\gamma_{k+1}^{(i)}|x_{k+1},\mathcal{Y}_{k+1}}(B_{k+1}^{(i)},\Gamma_{k+1}^{(i)} \mid X_{k+1},\Upsilon_{k+1}) \qquad (80)
\end{aligned}
$$

which yields (23a) written for the time instant $k+1$.

APPENDIX B. PROOF OF PROPOSITION 2

The proof is based on the following lemmas.

LEMMA 1 *Given the fault indicator γ_{k+1} and the measurement history $\mathcal{Y}_{k+1}$, the joint distribution of x_{k+1} and b_{k+1} is Gaussian.*

PROOF The lemma follows from Assumption 2 and the facts that given the fault indicators 1) the measurement vector y_{k+1} is a linear function of the state vectors x_{k+1} and b_{k+1}, and 2) the measurement noises $v_{k+1}^{(i)}$ are all Gaussian.

LEMMA 2 *The distributions $x_{k+1} \mid \mathcal{Y}_k$ and $x_{k+1} \mid \mathcal{Y}_{k+1}$ are Gaussian.*

PROOF It follows from Assumption 2 that the marginal distribution $x_{k+1} \mid \gamma_{k+1}, \mathcal{Y}_k$ is Gaussian. But, due to Assumption 3, given the measurement history $\mathcal{Y}_k$, the main state vector x_{k+1} and the fault vector γ_{k+1} are independent, hence $x_{k+1} \mid \mathcal{Y}_k$ is Gaussian. Similarly, due to Lemma 1, $x_{k+1} \mid \gamma_{k+1}, \mathcal{Y}_{k+1}$ is Gaussian. The independence of x_{k+1} and γ_{k+1} given $\mathcal{Y}_{k+1}$ renders $x_{k+1} \mid \mathcal{Y}_{k+1}$ Gaussian.

LEMMA 3 *The distributions $x_{k+1}, b_{k+1}^{(i)} \mid \gamma_{k+1}^{(i)}, \mathcal{Y}_k$ and $x_{k+1}, b_{k+1}^{(i)} \mid \gamma_{k+1}^{(i)}, \mathcal{Y}_{k+1}$ are Gaussian.*

PROOF First, according to Assumption 2, $x_{k+1}, b_{k+1} \mid \gamma_{k+1}, \mathcal{Y}_k$ is Gaussian. Therefore, $x_{k+1}, b_{k+1}^{(i)} \mid \gamma_{k+1}, \mathcal{Y}_k$ is also Gaussian. But using Assumption 3 and Proposition 1 yields

$$
\begin{aligned}
&p_{x_{k+1},b_{k+1}|\gamma_{k+1},\mathcal{Y}_k}(X_{k+1}, B_{k+1} \mid \Gamma_{k+1}, \Upsilon_k) \\
&\quad = \frac{p_{b_{k+1},\gamma_{k+1}|x_{k+1},\mathcal{Y}_k}(B_{k+1}, \Gamma_{k+1} \mid X_{k+1}, \Upsilon_k) p_{x_{k+1}|\mathcal{Y}_k}(X_{k+1} \mid \Upsilon_k)}{p_{\gamma_{k+1}|\mathcal{Y}_k}(\Gamma_{k+1} \mid \Upsilon_k)} \\
&\quad = \frac{p_{b_{k+1},\gamma_{k+1}|x_{k+1},\mathcal{Y}_k}(B_{k+1}, \Gamma_{k+1} \mid X_{k+1}, \Upsilon_k) p_{x_{k+1}|\gamma_{k+1}^{(i)},\mathcal{Y}_k}(X_{k+1} \mid \Gamma_{k+1}^{(i)}, \Upsilon_k)}{p_{\gamma_{k+1}|x_{k+1},\mathcal{Y}_k}(\Gamma_{k+1} \mid X_{k+1}, \Upsilon_k)} \\
&\quad = p_{x_{k+1}|\gamma_{k+1}^{(i)},\mathcal{Y}_k}(X_{k+1} \mid \Gamma_{k+1}^{(i)}, \Upsilon_k) \prod_{j=1}^{m} p_{b_{k+1}^{(j)}|\gamma_{k+1}^{(j)},x_{k+1},\mathcal{Y}_k}(B_{k+1}^{(j)} \mid \Gamma_{k+1}^{(j)}, X_{k+1}, \Upsilon_k). \qquad (81)
\end{aligned}
$$

Therefore

$$
\begin{aligned}
&p_{x_{k+1},b_{k+1}^{(i)}|\gamma_{k+1},\mathcal{Y}_k}(X_{k+1}, B_{k+1}^{(i)} \mid \Gamma_{k+1}, \Upsilon_k) \\
&\quad = p_{x_{k+1}|\gamma_{k+1}^{(i)},\mathcal{Y}_k}(X_{k+1} \mid \Gamma_{k+1}^{(i)}, \Upsilon_k) \\
&\qquad \times p_{b_{k+1}^{(i)}|\gamma_{k+1}^{(i)},x_{k+1},\mathcal{Y}_k}(B_{k+1}^{(i)} \mid \Gamma_{k+1}^{(i)}, X_{k+1}, \Upsilon_k) \\
&\quad = p_{x_{k+1},b_{k+1}^{(i)}|\gamma_{k+1}^{(i)},\mathcal{Y}_k}(X_{k+1}, B_{k+1}^{(i)} \mid \Gamma_{k+1}^{(i)}, \Upsilon_k). \qquad (82)
\end{aligned}
$$

The pdf on the left hand side is Gaussian and so is the pdf on the right hand side. The fact that $x_{k+1}, b_{k+1}^{(i)} \mid \gamma_{k+1}^{(i)}, \mathcal{Y}_{k+1}$ is Gaussian can be shown similarly using Lemma 1.

APPENDIX C. PROOF OF PROPOSITION 3

The result (45) follows from Bayes' law and the fact that, according to (44),

$$
\begin{aligned}
&p_{y^{(r)}|x,y^{(1)},y^{(2)},\ldots,y^{(r-1)}}(Y^{(r)} \mid X, Y^{(1)}, Y^{(2)}, \ldots, Y^{(r-1)}) \\
&\quad = p_{y^{(r)}|x}(Y^{(r)} \mid X). \qquad (83)
\end{aligned}
$$

The results (47) and (48) are established as follows

$$
\begin{aligned}
&p_{y^{(r)}|x,z^{(r)},y^{(1)},\ldots,y^{(r-1)}}(Y^{(r)} \mid X, Z^{(r)}, Y^{(1)}, \ldots, Y^{(r-1)}) \\
&\quad = \frac{p_{y^{(1)},\ldots,y^{(r)}|x,z^{(r)}}(Y^{(1)}, \ldots, Y^{(r)} \mid X, Z^{(r)})}{p_{y^{(1)},\ldots,y^{(r-1)}|x,z^{(r)}}(Y^{(1)}, \ldots, Y^{(r-1)} \mid X, Z^{(r)})}. \qquad (84)
\end{aligned}
$$

But, according to (46),

$$
\begin{aligned}
&p_{y^{(1)},\ldots,y^{(r)}|x,z^{(r)}}(Y^{(1)}, \ldots, Y^{(r)} \mid X, Z^{(r)}) \\
&\quad = \int_{-\infty}^{+\infty} p_{y^{(1)},\ldots,y^{(r)}|x,z^{(1)},\ldots,z^{(r)}}(Y^{(1)}, \ldots, Y^{(r)} \mid X, Z^{(1)}, \ldots, Z^{(r)}) \\
&\qquad \times p_{z^{(1)},\ldots,z^{(r-1)}|x,z^{(r)}}(Z^{(1)}, \ldots, Z^{(r-1)} \mid X, Z^{(r)}) dZ^{(1)} \cdots dZ^{(r-1)} \\
&\quad = \int_{-\infty}^{+\infty} \left(\prod_{i=1}^{r} p_{y^{(i)}|x,z^{(i)}}(Y^{(i)} \mid X, Z^{(i)}) \right) \\
&\qquad \times \left(\prod_{i=1}^{r-1} p_{z^{(i)}|x}(Z^{(i)} \mid X) \right) dZ^{(1)} \cdots dZ^{(r-1)} \\
&\quad = p_{y^{(r)}|x,z^{(r)}}(Y^{(r)} \mid X, Z^{(r)}) \prod_{i=1}^{r-1} p_{y^{(i)}|x}(Y^{(i)} \mid X). \qquad (85)
\end{aligned}
$$

Similarly,

$$
p_{y^{(1)},\ldots,y^{(r-1)}|x,z^{(r)}}(Y^{(1)}, \ldots, Y^{(r-1)} \mid X, Z^{(r)}) = \prod_{i=1}^{r-1} p_{y^{(i)}|x}(Y^{(i)} \mid X). \qquad (86)
$$

Substituting (85) and (86) into (84) yields

$$p_{y^{(r)}|x,z^{(r)},y^{(1)},\ldots,y^{(r-1)}}(Y^{(r)} \mid X,Z^{(r)},Y^{(1)},\ldots,Y^{(r-1)}) = p_{y^{(r)}|x,z^{(r)}}(Y^{(r)} \mid X,Z^{(r)}). \quad (87)$$

Now,

$$p_{z^{(r)}|x,y^{(1)},\ldots,y^{(r-1)}}(Z^{(r)} \mid X,Y^{(1)},\ldots,Y^{(r-1)}) = \frac{p_{y^{(1)},\ldots,y^{(r-1)}|x,z^{(r)}}(Y^{(1)},\ldots,Y^{(r-1)} \mid X,Z^{(r)})p_{z^{(r)}|x}(Z^{(r)} \mid X)}{p_{y^{(1)},\ldots,y^{(r-1)}|x}(Y^{(1)},\ldots,Y^{(r-1)} \mid X)} = p_{z^{(r)}|x}(Z^{(r)} \mid X) \quad (88)$$

which is (47). Finally, the result (48) follows from Bayes' law, (87) and (88).

REFERENCES

[1] White, N. A., Maybeck, P. S., and DeVilbiss, S. L.
Detection of interference/jamming and spoofing in a DGPS-aided inertial system.
IEEE Transactions on Aerospace and Electronic Systems, **34**, 4 (Oct. 1998), 1208–1217.

[2] Wertz, J. R.
Spacecraft Attitude Determination and Control.
Dordrecht: Reidel, 1978.

[3] Tugnait, J. K.
Detection and estimation for abruptly changing systems.
Automatica, **18**, 5 (1982), 607–615.

[4] Zhang, Y., and Li, X. R.
Detection and diagnosis of sensor and actuator failures using IMM estimator.
IEEE Transactions on Aerospace and Electronic Systems, **34**, 4 (Oct. 1998), 1293–1313.

[5] Ackerson, G. A., and Fu, K. S.
On state estimation in switching environments.
IEEE Transactions on Automatic Control, **AC-15**, 1 (Feb. 1970), 10–17.

[6] Nahi, N. E.
Optimal recursive estimation with uncertain observations.
IEEE Transactions on Information Theory, **IT-15** (July 1969), 457–462.

[7] Jaffer, A. G., and Gupta, S.
Optimal sequential estimation of discrete processes with Markov interrupted observations.
IEEE Transactions on Automatic Control, **AC-16**, 5 (Oct. 1971), 471–475.

[8] Blom, H. A. P., and Bar-Shalom, Y.
The interacting multiple model algorithm for systems with Markovian switching coefficients.
IEEE Transactions on Automatic Control, **33**, 8 (Aug. 1988), 780–783.

[9] Costa, O. L. V.
Minimum mean square error estimator for discrete-time Markovian linear systems.
IEEE Transactions on Automatic Control, **AC-39**, 8 (Aug. 1994), 1685–1689.

[10] de Freitas, N.
Rao-Blackwellised particle filtering for fault diagnosis.
In *Proceedings of 2002 IEEE Aerospace Conference*, Big Sky, MT, Mar. 2002, 4-1767–4-1772.

[11] Carlson, N. A.
Federated filter for fault-tolerant integrated navigation systems.
In *IEEE PLANS, Position Location and Navigation Symposium*, Dec. 1988, pp. 110–119.

[12] Brumback, B. D., and Srinath, M. D.
A fault-tolerant multisensor navigation system design.
IEEE Transactions on Aerospace and Electronic Systems, **AES-23**, 6 (Nov. 1987), 738–755.

[13] Rapoport, I., and Oshman, Y.
Optimal filtering in the presence of faulty measurement biases.
In *Proceedings of the 41st IEEE Conference on Decision and Control*, Las Vegas, NV, Dec. 2002, 2236–2241.

[14] Kaplan, M. H.
Modern Spacecraft Dynamics and Control.
New York: Wiley, 1976.

Ilia Rapoport was born in Ufa, USSR in January 1971. He received his B.Sc. (summa cum laude), M.Sc., and Ph.D. degrees in aerospace engineering from the Technion–Israel Institute of Technology, Haifa, Israel, in 1994, 2000, and 2005, respectively.

From 1995 to 2001 he served as an aerospace engineer in the Israeli Air Force. In 2005 he joined the Control and Navigation Group at El-Op, Electro-Optics Industries, Ltd. His research interests include estimation theory, random processes theory, fault detection and isolation, hybrid systems, satellite and inertial navigation.

Yaakov Oshman (A'96—SM'97—F'07) received his B.Sc. (summa cum laude) and D.Sc. degrees, both in aeronautical engineering, from the Technion–Israel Institute of Technology, Haifa, Israel, in 1975 and 1986, respectively.

From 1975 to 1981 he was with the Israeli Air Force, where he worked in the areas of structural dynamics and flutter analysis and flight testing. In 1987 he was a research associate at the Department of Mechanical and Aerospace Engineering of the State University of New York at Buffalo, where he was, in 1988, a visiting professor. Since 1989 he has been with the Department of Aerospace Engineering at the Technion–Israel Institute of Technology, where he is a professor and holder of the Louis and Helen Rogow Chair in Aeronautical Engineering.

Dr. Oshman is a member of the Technion's Asher Space Research Institute. He headed the Technion's Philadelphia Flight Control Laboratory (1993–1996). During the 1996/7 and 1997/8 academic years he spent a sabbatical with the Guidance, Navigation and Control Center of NASA's Goddard Space Flight Center, where he worked in research and development of spacecraft attitude estimation algorithms. He has consulted to RADA Electronic Industries Ltd., RAFAEL Ltd., and the Israeli Ministry of Defense. His research has been supported by the Israeli Aircraft Industries, the Israeli Ministry of Defense, the U.S. Air Force Office of Scientific Research (AFOSR), RAFAEL Ltd., and the Israeli Science Foundation (ISF), as well as by various Technion research grants. His research interests are in advanced optimal estimation, information fusion and control methods and their application in Aerospace guidance, navigation and control systems. Of particular interest are interdisciplinary aerospace systems, including structural estimation and control, and health monitoring/fault detection and isolation (FDI) systems.

Dr. Oshman is the President of the Israeli Association for Automatic Control, a national member organization of the International Federation of Automatic Control (IFAC). He is a member of the AIAA Guidance, Navigation and Control Technical Committee. He has published over 130 journal and conference papers, five book chapters, and numerous technical reports in these areas. He is a coauthor of the paper that was awarded the Best Paper Award of the 2002 AIAA Astrodynamics Specialist Conference, and a coauthor and advisor of the paper that was awarded the Best Paper Award of the 2004 AIAA Guidance, Navigation and Control Conference. He received the Technion's Raymond and Miriam Klein Research Prize for his research on enhanced air-to-air missile tracking using target orientation observations (2002), and the Technion's Meir Hanin Research Prize for his work on spacecraft angular velocity estimation (2004). The latter work has been put to use in the Israeli AMOS-2 communication satellite. He has been on the program committees of over a dozen international conferences.

Dr. Oshman is a technical editor for Guidance and Control Systems for the *IEEE Transactions on Aerospace and Electronic Systems*, and an international advisor (member of the editorial board) of the *AIAA Journal of Guidance, Control and Dynamics*. He is an Associate Fellow of the AIAA.